




Persistent metagenomic signatures of early-life hospitalization and antibiotic treatment in the infant gut microbiota and resistome

Andrew J. Gasparrini¹ , Bin Wang^{1,2}, Xiaoqing Sun^{1,2}, Elizabeth A. Kennedy¹, Ariel Hernandez-Leyva¹, I. Malick Ndao³, Phillip I. Tarr^{3,4} , Barbara B. Warner³ and Gautam Dantas^{1,2,4,5*} 

Hospitalized preterm infants receive frequent and often prolonged exposures to antibiotics because they are vulnerable to infection. It is not known whether the short-term effects of antibiotics on the preterm infant gut microbiota and resistome persist after discharge from neonatal intensive care units. Here, we use complementary metagenomic, culture-based and machine learning techniques to study the gut microbiota and resistome of antibiotic-exposed preterm infants during and after hospitalization, and we compare these readouts to antibiotic-naïve healthy infants sampled synchronously. We find a persistently enriched gastrointestinal antibiotic resistome, prolonged carriage of multidrug-resistant Enterobacteriaceae and distinct antibiotic-driven patterns of microbiota and resistome assembly in extremely preterm infants that received early-life antibiotics. The collateral damage of early-life antibiotic treatment and hospitalization in preterm infants is long lasting. We urge the development of strategies to reduce these consequences in highly vulnerable neonatal populations.

Gut microbes have important functions in host health and disease throughout life, particularly during infancy¹. Infant gut microbiota (IGM) assembly is accelerated during the first months of life, following inoculation with organisms from mothers and the environment², but stabilizes by approximately three years of age³. Treatment with antibiotics during this interval may disproportionately damage the host–microbiota ecosystem^{3–5}. Indeed, emerging data suggest that early-life gut microbial alterations correlate with chronic metabolic and immune disorders later in life^{1,4,6–16}, including allergies¹⁷, psoriasis¹⁸, adiposity¹⁹, diabetes²⁰ and inflammatory bowel disease^{21–23}. For most of these disorders, a causal link between antibiotic-mediated microbiota disruption and onset of pathology is lacking. However, antibiotic treatment during infancy is associated with permanent immune alterations^{18,24} and inflammatory bowel disease in childhood²³, highlighting the damaging long-term potential of early-life antibiotic treatment.

Over 11% of live births worldwide occur preterm²⁵, and preterm birth and its sequelae are prominent causes of childhood morbidity and mortality worldwide²⁶. As bacterial infections are frequent complications of preterm birth²⁷, 79% of very-low birthweight and 87% of extremely low birthweight infants in neonatal intensive care units (NICUs) in the United States receive antibiotics within 3 d of birth²⁸. Even in healthy infants, the gastrointestinal tract harbours a diverse antibiotic resistome²⁹, which is shaped by factors including antibiotics, diet and environment^{30–32}. Preterm IGM perturbation immediately following antibiotic treatment is characterized by decreased alpha diversity, increased Enterobacteriaceae abundance and antibiotic-specific enrichment of antibiotic-resistance genes (ARGs) and multidrug-resistant organisms (MDROs)³³. As microbiota perturbation during infancy may be disproportionately damaging^{34,35}, it is imperative to study the lasting effects of antibiotics and hospitalization on

the preterm IGM. Previous studies of preterm infants report IGM recovery that is concomitant with NICU discharge^{36–38}. However, these studies rely on culture or amplicon sequencing (for example, 16S rRNA) based analyses focussing on the taxa found in the microbiota rather than the functions that they collectively encode. Here we analyse ~1.2 Tb of metagenomic DNA from 437 infant stools, culture and sequence 530 bacterial isolates, and functionally select 300 Gb of metagenomic DNA for antibiotic resistance to investigate the long-term consequences of antibiotic treatment on the preterm IGM.

The effect of antibiotics on the preterm IGM

To understand the long-term effects of prematurity and associated early-life hospitalization and antibiotic therapy on the IGM, we performed whole-metagenome shotgun sequencing of 437 faecal samples from 58 infants throughout the first 21 months of life (Supplementary Figs. 1 and 2). Our cohort included 41 preterm infants who were sampled at the NICU of St Louis Children's Hospital and after being discharged to home. One subset of this cohort ($n=9$) received scant antibiotic therapy neonatally (each received a single concurrent course of gentamicin and ampicillin for less than 7 d). The remaining 32 preterm infants received extensive antibiotic treatment over the first 21 months (median (interquartile range (IQR)) 8 courses (6, 10.3) and 29.5 d (41.63 d, 68.3 d) antibiotic therapy). All of the infants in this cohort were classified as being born preterm ((median (IQR) gestational age at birth of 26 weeks (25, 27)) with very low birth weights (median (IQR) 840 g (770 g, 960 g)). Furthermore, we included 17 antibiotic-naïve, healthy early term³⁹ or late-preterm⁴⁰ (median (IQR) gestational age at birth 36 weeks (36, 37 weeks); near-term) infants of the same chronological age range, sampled synchronously with the preterm cohort.

¹The Edison Family Center for Genome Sciences and Systems Biology, Washington University in St Louis School of Medicine, St Louis, MO, USA. ²Department of Pathology and Immunology, Washington University in St Louis School of Medicine, St Louis, MO, USA. ³Department of Pediatrics, Washington University in St Louis School of Medicine, St Louis, MO, USA. ⁴Department of Molecular Microbiology, Washington University in St Louis School of Medicine, St Louis, MO, USA. ⁵Department of Biomedical Engineering, Washington University in St Louis, St Louis, MO, USA. *e-mail: dantas@wustl.edu

We inferred bacterial taxonomic composition using MetaPhlAn2⁴¹. Across all of the infants, Shannon diversity increased during a developmental phase before stabilizing (Fig. 1a). In near-term infants, the Shannon diversity of the microbiota increases rapidly during the first month before plateauing, whereas the diversity of the preterm-infant microbiota increases more gradually and with greater variation (Fig. 1a). Enterobacteriaceae and Enterococcaceae dominate the preterm IGM during the first months of life. By contrast, early colonization by Enterobacteriaceae in near-term infants precedes robust colonization with Bifidobacteriaceae (Fig. 1b, Supplementary Fig. 3). Enterococcaceae is significantly less abundant early in life (<4 months chronological age) in near-term compared with preterm infants ($P < 0.001$, Wilcoxon rank sum), and Prevotellaceae is similarly less abundant later during infancy (>8 months chronological age) in preterm infants compared with near-term infants ($P < 1 \times 10^{-10}$, Wilcoxon rank sum). Despite these differences, we observed predicted functional stability of the microbiota both over time and between groups (Fig. 1c), as inferred by HUMAnN2⁴². Although it is probable that greater variation exists when finer functional categories or predicted hosts of functions are taken into account, the invariability of microbiota functional capacity at this high level suggests that although prematurity, early-life hospitalization and antibiotic treatment substantially perturb the taxonomic composition of the microbiota, a core set of microbial functions remains conserved across hosts⁴³.

Low gut-microbiota diversity is often associated with adverse health in infants^{44–46}, children⁵ and adults⁴⁷. To identify features associated with microbiota diversity, we regressed Shannon diversity on clinical variables (see Methods; Supplementary Table 1) using a generalized linear mixed model with the subject defined as individual effect. All of the variables in Supplementary Table 1 were included in the initial modelling, and a final model was fit by backwards elimination of variables. After correcting for multiple comparisons, we found that day of life was significantly associated with increased Shannon diversity ($P < 0.001$), whereas recent (within 30 d of sample collection) administration of vancomycin ($P < 0.001$), ampicillin ($P < 0.001$), meropenem ($P = 0.009$) or cefepime ($P = 0.012$) was significantly associated with decreased diversity (Fig. 1d). No clinical variable included in the model other than antibiotic treatment was significantly associated with IGM diversity. The sparse model explained 57% of the variance in Shannon diversity by the fixed effects (day of life and antibiotic treatments) alone, and an additional 12% by subject. The magnitude of the model estimate for day of life (0.002) was substantially less than those for recent antibiotics (vancomycin, -0.34 ; ampicillin, -0.60 ; meropenem, -0.42 ; cefepime, -0.46 ; oxacillin, -0.70). Thus, a single recent course of antibiotics has an effect on diversity of the same magnitude as the diversity increase observed over around 5–12 months of life. Across all of the infants in our cohort through the first 110 d of life, the Shannon diversity of the microbiota was significantly lower in infants who received more than one course of antibiotics in the previous month (Fig. 1e). Accordingly, recent antibiotic treatment seems to be a key driver of microbiota diversity early in life.

Partial microbiota recovery following NICU discharge

Although the taxonomic composition of the preterm infant microbiota clustered by both gestational age at birth and antibiotic treatment status (Adonis test, $P < 0.001$, Bray–Curtis distance), chronological age was a major driver of microbiota composition across all infants (Fig. 2a). We hypothesized that after observed early-life perturbation, the composition of the preterm microbiota would converge towards that of age-matched healthy, antibiotic-naïve near-term infants within the first 21 months of life, but that microbiota ‘scars’ from this early-life disruption (for example, enriched ARGs and MDROs) would persist.

To quantify the extent of this perturbation, we used random forests to regress the relative abundances of species in the microbiota of infants against their chronological age as previously described⁴⁸. The minimum number of variables required for accurate prediction was 50 (Fig. 2b). We trained a model consisting of the 50 most informative predictors on the subset of antibiotic-naïve near-term infants to model healthy microbiota development, and subsequently refined and validated the model. The top age-discriminatory taxa in the IGM of antibiotic-naïve near-term infants were *Faecalibacterium prausnitzii*, *Subdoligranulum* sp., *Ruminococcus gnavus* and *Oscillobacter* sp. (Fig. 2c). We used this sparse model to predict infant chronological age using the relative abundance of these 50 species. This prediction—or ‘microbiota age’—approximates relative microbiota maturity⁴⁸. We observed a linear relationship between the chronological and microbiota ages of antibiotic-naïve near-term infants, suggesting that the model accurately predicts the age of near-term infants. However, for preterm infants, predicted microbiota ages were younger than chronological age across several stages of development, indicating that microbiota development is disrupted in these infants. To better quantify the extent of disruption, we computed a microbiota-for-age z -score (MAZ) for each metagenome, as previously described⁴⁸. Using a z -score to compare age bins is necessary because this value reflects the variance of the predicted age across the development of infant microbiota. Preterm infants who receive antibiotic treatment have significantly lower MAZ values than near-term infants in the first months of life (Fig. 2e). However, by months 12–15 of life, the MAZ values of hospitalized preterm infants closely resemble those of healthy antibiotic-naïve near-term infants (Fig. 2f). Thus, despite transient delays in the development of the preterm IGM, the bacterial taxonomic composition converges to common structures with those of healthy antibiotic-naïve infants within the first 21 months of life (Fig. 2d).

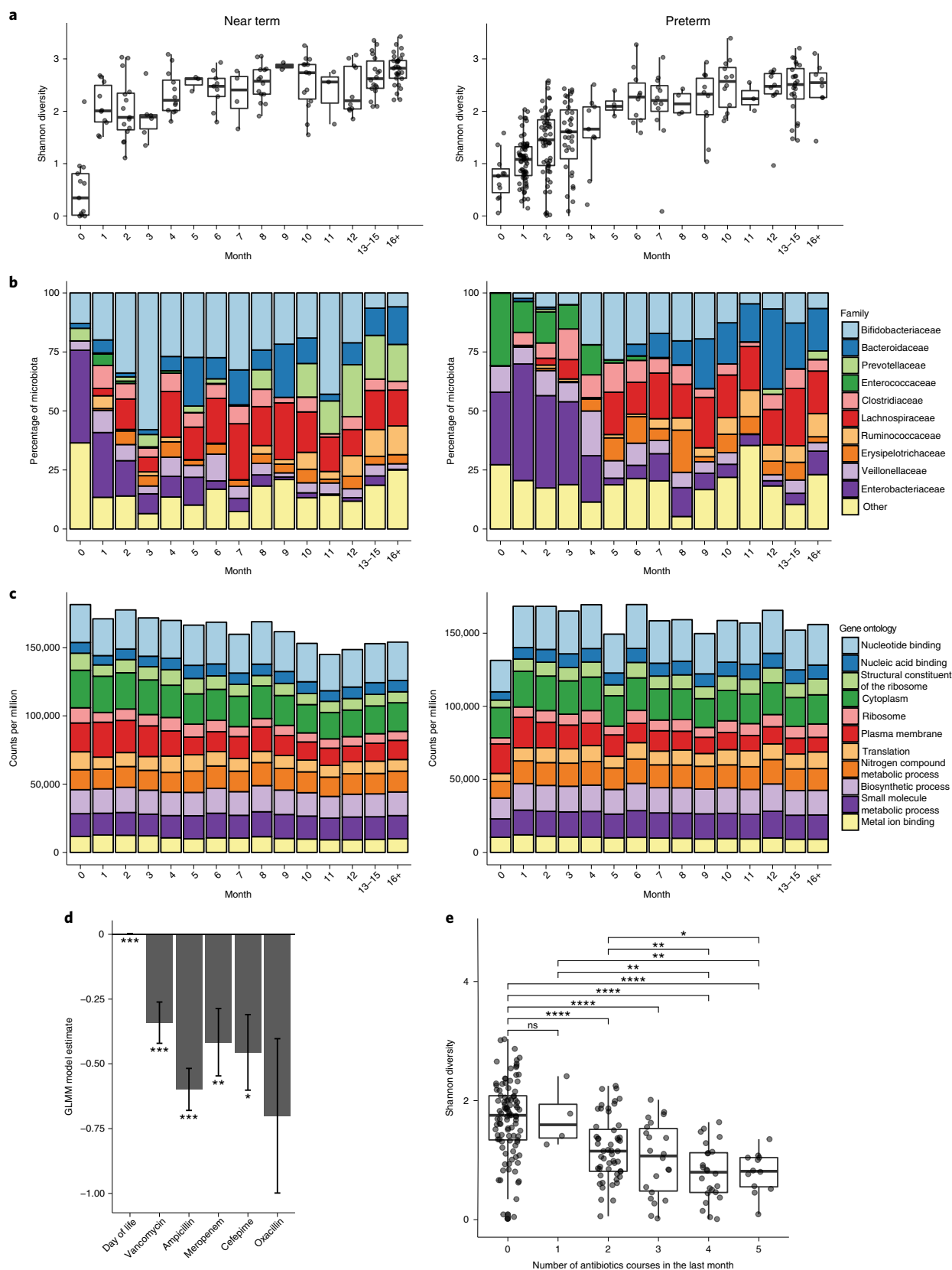
Antibiotic resistome of preterm IGM

We next characterized the antibiotic resistome encoded in the IGM of our cohort. We conducted functional metagenomic analysis⁴⁹ of 217 preterm- and term-infant stools, selected to encompass the diversity in clinical variables in our cohort. We constructed 22 functional metagenomic libraries totalling 396 Gb (Supplementary Fig. 4, Supplementary Table 1; see Methods) with an average insert size of 2–3 kb, selected libraries on 16 antibiotics relevant to infants and children (Supplementary Table 3), and we recovered resistant transformants for each antibiotic except for meropenem (Supplementary

Fig. 1 | Clinical variables predict microbiota diversity and composition. **a**, Shannon diversity of all near-term ($n = 17$) and preterm ($n = 41$) infants in this study, shown by month of life. **b**, Microbiota species and functional compositions inferred by MetaPhlAn2 of all near-term ($n = 17$) and preterm ($n = 41$) infants in this study. **c**, Microbiota species and functional compositions inferred by HUMAnN2 of all near-term ($n = 17$) and preterm ($n = 41$) infants in this study. **d**, Day of life is significantly associated with an increase in microbiota Shannon diversity, whereas vancomycin, ampicillin, meropenem or cefepime treatment within the month before sampling is associated with significantly decreased species richness. *** $P < 0.001$; ** $P < 0.01$; * $P < 0.05$; generalized linear mixed model with subject as random effect using 437 infant gut metagenomes. Oxacillin was included in the model but was not significant after correction for multiple comparisons. Error bars indicate s.e.m. **e**, Shannon diversity is significantly lower in infants who received more than one course of antibiotic treatment in the past month compared with infants who had not received antibiotic treatment during that time period. **** $P < 0.0001$; ns, not significant; statistical analysis was performed using two-sided Wilcoxon rank sum tests with Benjamini–Hochberg correction; $n = 212$ samples. For box plots, data are the first quartile, median and third quartile of the data with whiskers extending to the last data point within $1.5 \times$ the interquartile range.

Fig. 4). We found that the infant gut metagenome encoded transferable resistance even to antibiotics that are rarely or never used in neonates, such as ciprofloxacin and chloramphenicol, and those that represent last lines of defence against MDROs, such as

tigecycline and colistin. Only one of eight libraries constructed from stools of antibiotic-naïve near-term infants encoded ciprofloxacin resistance (mediated by loci other than *gyrA* or *parC*), whereas six out of fourteen libraries constructed from preterm-infant stools



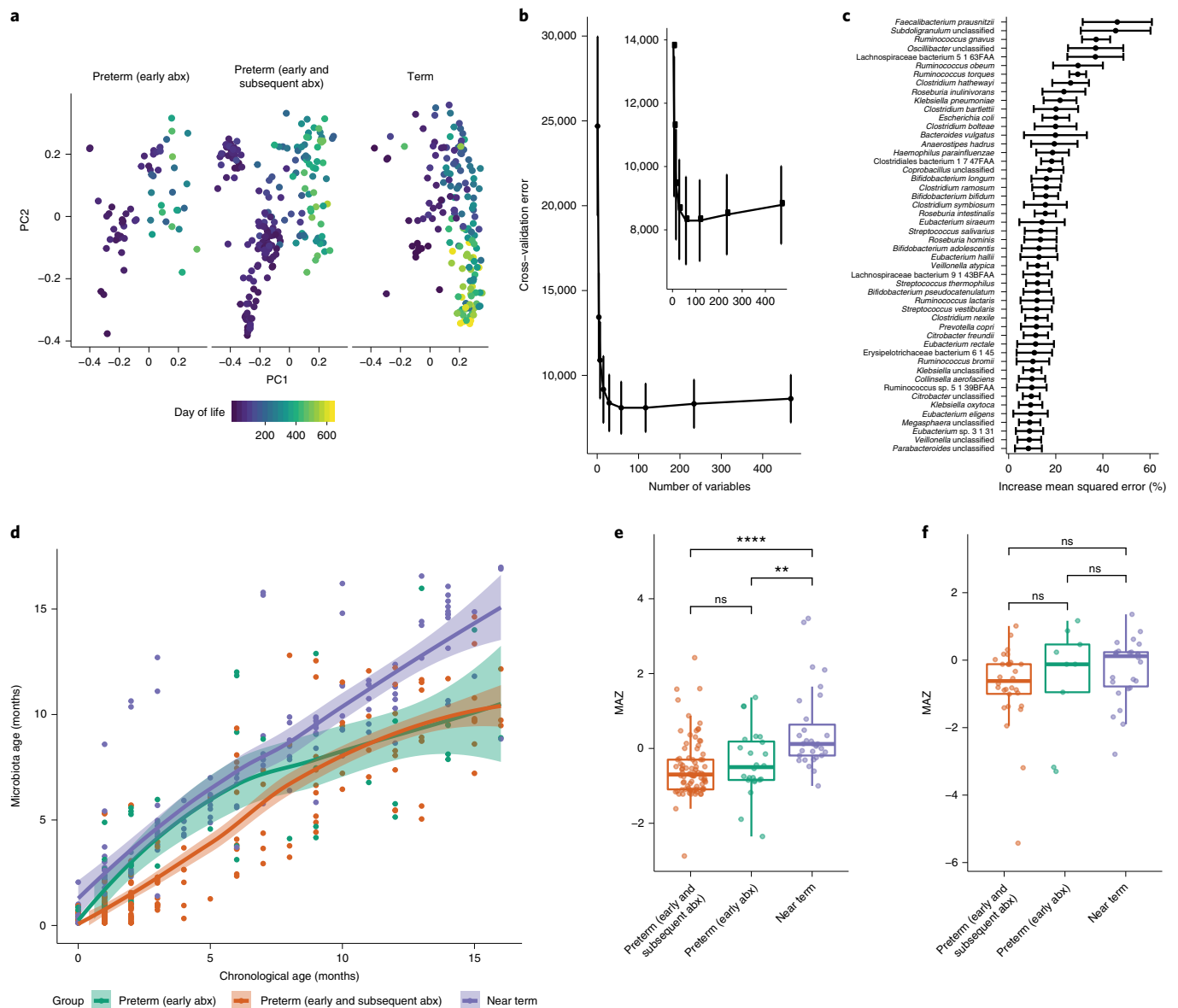


Fig. 2 | Partial architectural recovery of preterm IGM following discharge from NICU. a, Microbiota composition is distinct between near-term infants, preterm infants with early only antibiotic treatment and preterm infants with early and subsequent antibiotic treatment (Bray–Curtis distance; $P < 0.001$; Adonis test, $n = 437$ samples), but chronological day of life is a major driver of microbiota composition. abx, antibiotics. PC1 and PC2 refer to first and second principal component analysis scores, respectively. **b**, Fivefold cross-validation indicates that 50 variables are sufficient for random forest predictions of the chronological age of near-term infants on the basis of microbiota composition. The inset details vertex. Data are mean \pm s.e.m. computed over 100 iterations. **c**, The 50 most informative predictors to the random forest model. These species were included in a sparse model. Data are mean \pm s.e.m. computed over 100 iterations. **d**, The sparse random forest model accurately predicts the chronological age of near-term infants, but the chronological age of preterm infants was predicted to be less than the actual age across numerous stages of development. Curves are fit to each group using loess regression, and shading indicates the 95% confidence interval; $n = 437$ samples. **e**, Preterm-infant MAZ is significantly lower than that of near-term infants in the first month of life, indicating early microbiota immaturity. $^{**}P < 0.01$; $^{****}P < 0.0001$; ns, not significant; statistical analyses were performed using two-sided Wilcoxon rank sum tests; $n = 140$ samples. **f**, Preterm infant MAZ is statistically indistinguishable from that of near-term infants by 12–15 months of life, indicating resolution of microbiota immaturity by this time point ($P > 0.05$). ns, not significant; statistical analysis was performed using a two-sided Wilcoxon rank sum test; $n = 65$ samples. For the box plots, data are the first quartile, median and third quartile of the data with whiskers extending to the last data point within $1.5 \times$ the interquartile range.

encoded ciprofloxacin resistance. This observation, given the scarce use of ciprofloxacin in neonates⁵⁰, suggests that either acquired (as opposed to intrinsic) ciprofloxacin resistance occurs naturally in preterm infant gut bacterial communities, or that organisms resistant to ciprofloxacin are co-selected by other antibiotics to which they are resistant.

We sequenced resistance-conferring metagenomic inserts and assembled 874 unique ARGs. The median identity of these functionally selected ARGs to the NCBI non-redundant protein database was 94.4%, whereas their median identity to the Comprehensive Antibiotic Resistance Database (CARD) entries⁵¹ was 32.0% (Fig. 3a). Therefore, although most resistance determinants discovered in our

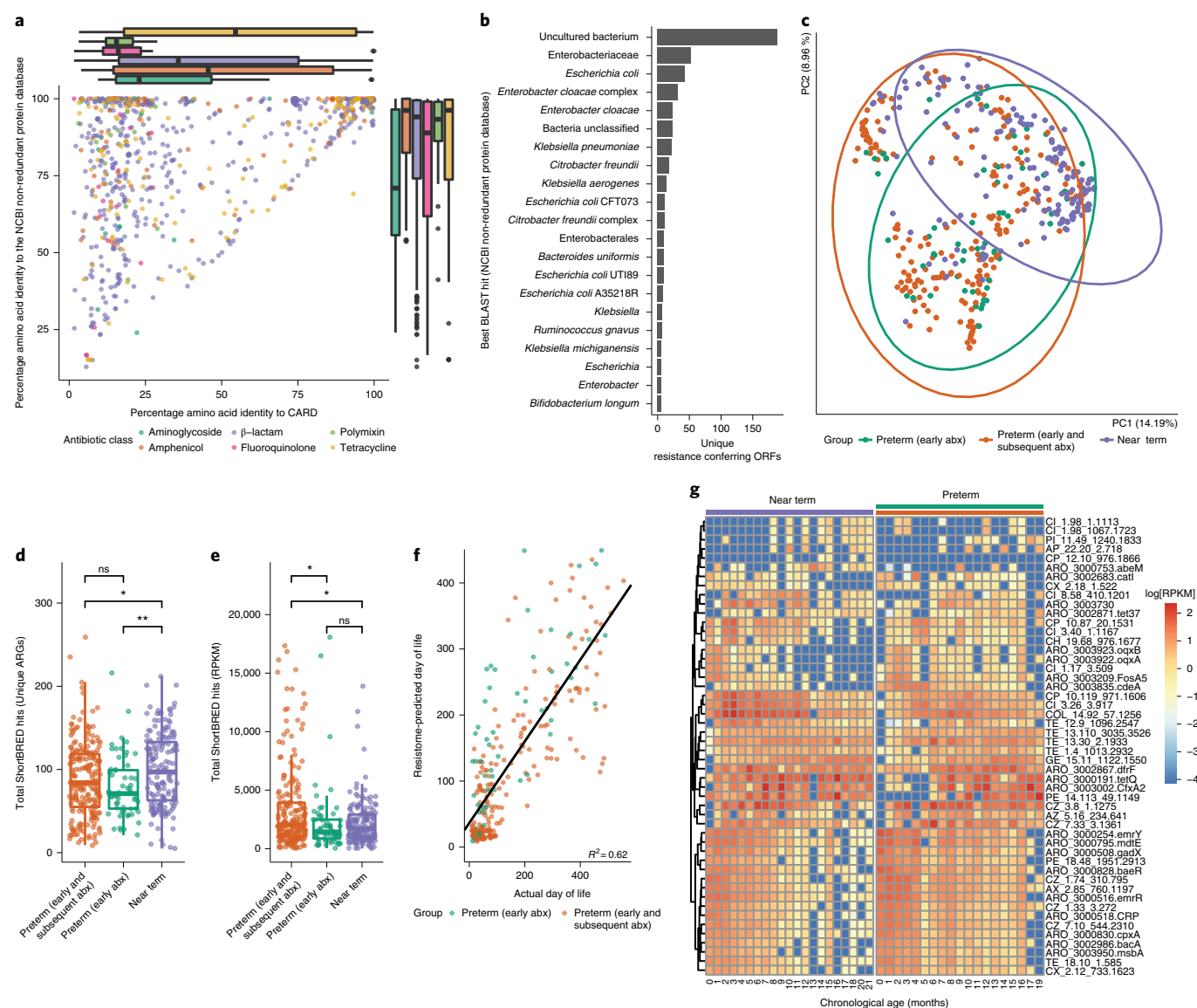


Fig. 3 | Preterm infants harbour an enriched gut resistome. **a**, Amino acid identity between all of the functionally selected ARGs and their top hit in CARD versus their top hit in the NCBI non-redundant protein database, coloured by class of antibiotic used for selection. Notably, ARGs recovered by fluoroquinolone and polymyxin selection have a very low median identity to CARD; $n=879$ ARGs. The grey dots indicate outliers in the boxplots, beyond 1.5x the interquartile range spanned by the whiskers. **b**, The most commonly predicted hosts of functionally selected ARGs on the basis of highest identity BLAST hits in the NCBI non-redundant protein database. **c**, Gut resistome composition is different between near-term infants, preterm infants with only early antibiotic treatment and preterm infants with early and subsequent antibiotic treatment (Bray–Curtis distance, $P<0.001$, Adonis test; $n=437$ samples). **d**, Preterm infants had fewer unique ARGs encoded in their gut metagenomes than near-term infants. * $P<0.05$; ** $P<0.01$; ns, not significant; statistical analysis was performed using a two-sided Wilcoxon rank sum test; $n=437$ samples. **e**, The cumulative resistome relative abundance was significantly higher in the gut microbiota of preterm infants with early and subsequent antibiotic treatment compared with both preterm infants with only early antibiotic treatment and near-term infants. * $P<0.05$; ns, not significant; statistical analysis was performed using two-sided Wilcoxon rank sum tests; $n=437$ samples. **f**, A random forest model trained on the gut resistome of preterm infants poorly predicts chronological age of near-term infants. The black line is the linear regression line of day of life, as predicted by the random forest model against the actual day of life ($R^2=0.62$); $n=437$ samples. **g**, Relative abundance of the 50 most informative resistance genes over the first months of life in near-term and preterm infants. Resistance genes are hierarchically clustered and listed to the right of the heat maps. The coloured bars above the heat maps correspond to the colours in **c–e**. For canonical resistance genes, the CARD accession is displayed, and for resistance genes that were functionally selected in this study, the relevant selection information is listed. For the box plots in **a,d,e**, data are the first quartile, median and third quartile of the data, with whiskers extending to the last data point within 1.5x the interquartile range.

functional selections have been previously sequenced, they have frequently not been assigned resistance functions—a discordance that we have previously noted³³. Functionally selected ARGs with a low identity to CARD entries, while not canonical resistance genes that are widespread in the clinical setting at this point, represent candidates for or progenitors of clinical resistance genes given

opportunity, mobilization or evolution^{49,52}. The predicted sources of resistance conferring open reading frames (ORFs) (determined by best BLAST hit to the NCBI non-redundant protein database) were predominantly uncultured bacteria or Enterobacteriaceae (Fig. 3b). The identification of Enterobacteriaceae as probable hosts of ARGs in the IGM is consistent with the current understanding

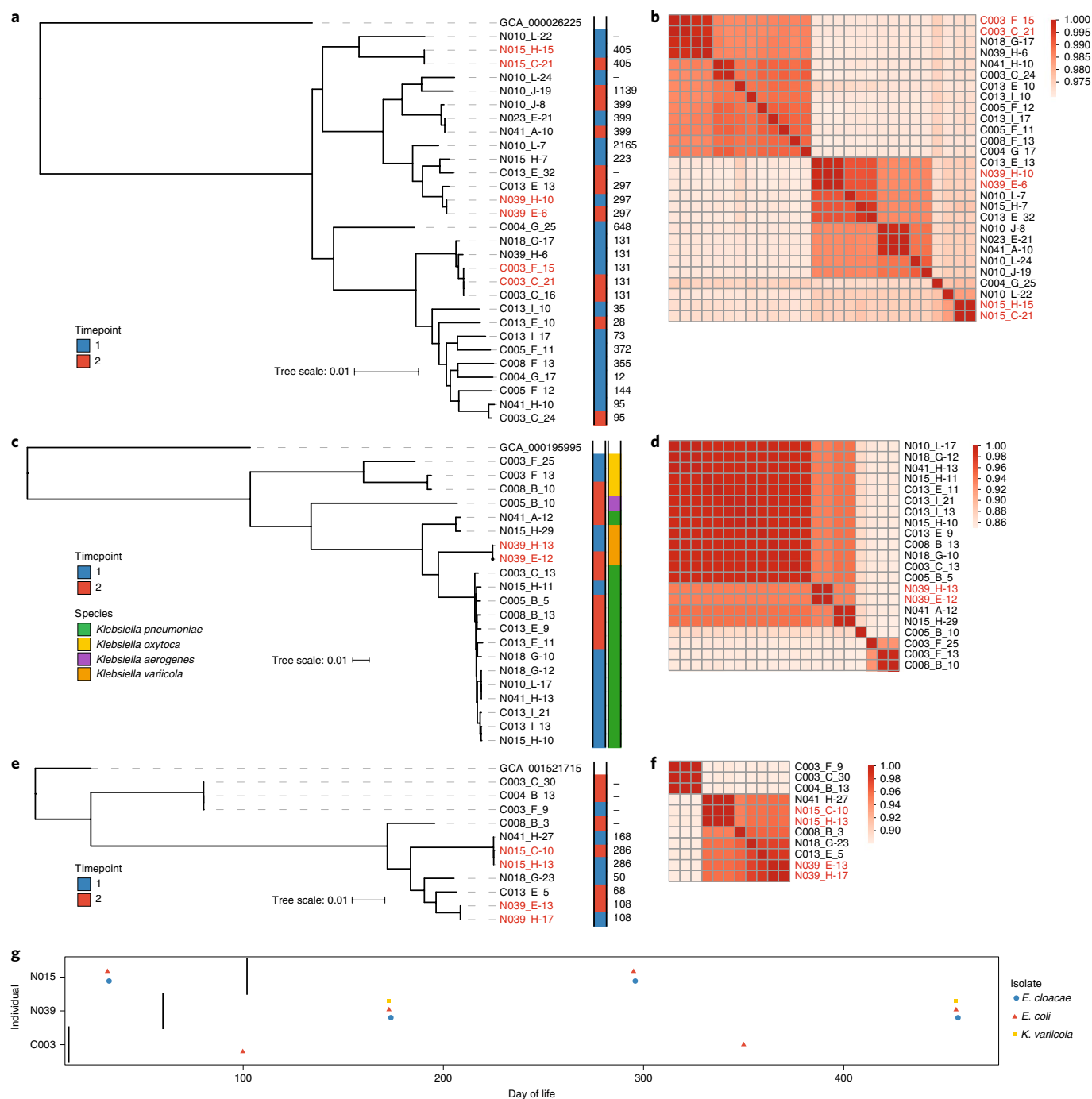


Fig. 4 | Multidrug-resistant Enterobacteriaceae lineages persist in IGM. **a,c,e**, Maximum-likelihood core-genome phylogenies of *E. coli* (**a**), *Klebsiella* spp. (**c**) and *E. cloacae* (**e**) isolated from infant stool samples. The annotations to the right of the metadata indicate timepoints of isolation and sequence type (determined by in silico multilocus sequence typing (MLST)) for *E. coli* and *E. cloacae* or by species for *Klebsiella*. Persistent isolates are highlighted in red. Timepoint 1 refers to the first sample cultured from an infant; timepoint 2 refers to the second sample (see Methods for details on culturing protocols). **b,d,f**, Average nucleotide identity (ANI) heat maps for *E. coli* (**b**), *Klebsiella* spp. (**d**) and *E. cloacae* (**f**) indicate that persistent isolates are isogenic—that is, they share more than 99.997% nucleotide identity. Persistent isolate pairs are highlighted in red. **g**, A timeline of isolation of persistent Enterobacteriaceae from infant stool samples. The vertical bars indicate the days on which the infants were discharged from the hospital. The first two infants displayed are preterm infants, whereas the third is a near-term infant.

of Enterobacteriaceae as prolific hosts and traffickers of ARGs^{53–55}. Moreover, the identification of uncultured (189 ORFs) and unclassified (24 ORFs) bacteria as sources of ARGs highlights the value of functional metagenomics as a culture- and sequence-unbiased method for characterizing resistomes⁵².

Highlighting the potential for lateral ARG exchange within the infant microbiome, 225 contigs (6.4% of all contigs) recovered in functional selections encoded a mobile genetic element (MGE; Supplementary Fig. 5a–e). MGEs were most frequently observed in tetracycline selections (Supplementary Fig. 5f) but were also

commonly observed in β -lactam, chloramphenicol, gentamicin and ciprofloxacin selections. We observed enrichment for MGEs on amoxicillin and clavulanate ($P < 0.01$, hypergeometric test), tetracycline ($P < 0.01$, hypergeometric test) and gentamicin ($P < 0.001$, hypergeometric test). The synteny of functionally selected ARGs with MGEs suggests the possibility of a mobilizable resistome in the IGM.

We extended our resistome analysis using ShortBRED⁵⁶ to quantify translated ARG abundance in all of the sequenced metagenomes with a custom database that included all of the ARGs from CARD as well as the functionally selected ARGs identified here. Resistomes clustered according to gestational age at birth and antibiotic-treatment status (Fig. 3c; $P < 0.001$, Adonis test). The gut metagenomes of preterm infants encoded fewer unique ARGs than those of near-term infants ($P < 0.01$, Wilcoxon rank sum; Fig. 3d). However, the cumulative resistome relative abundance was significantly higher in the IGM of preterm infants who received early and subsequent antibiotic treatment compared with preterm infants who received only early antibiotic treatment and antibiotic-naïve near-term infants ($P < 0.05$, Wilcoxon rank sum; Fig. 3e). There was a weak inverse correlation between taxonomic alpha diversity and cumulative resistome burden across all of the metagenomes ($R^2 = 0.09$; Supplementary Fig. 6a), indicating that resistome-enriched microbiota are dominated by a few species. Indeed, in 41 of the 54 metagenomes with a cumulative resistome of reads per kb per million mapped reads (RPKM) of more than 5000, a single species comprised more than 50% of the relative abundance of the microbiota. In 25 of these samples, the dominant species was *Escherichia coli* (Supplementary Fig. 6b). Other dominant species were *Enterococcus faecalis* ($n = 5$), *Klebsiella pneumoniae* ($n = 2$), *Staphylococcus epidermidis* ($n = 2$), *Enterobacter aerogenes* ($n = 2$), *Bifidobacterium breve* ($n = 2$), *Pseudomonas aeruginosa*, *Bifidobacterium longum* and *Citrobacter koseri* ($n = 1$ each). Thus, it seems that extreme prematurity and its associated hospitalization and antibiotic treatment select for one or two MDROs that dominate the IGM rather than enriching for a greater diversity of resistant organisms.

To define the developmental progression of the infant gastrointestinal resistome over the first months of life, we regressed the abundance of ARGs in a subset of antibiotic-naïve near-term infant gut metagenomes against the day of life for these infants using random forests⁵⁷. We constructed a sparse model using the 50 most informative ARGs. The sparse model was subsequently applied to preterm samples to predict 'resistome age'. A clear developmental trajectory on the basis of these 50 ARGs was evident in near-term infants (Fig. 3g). The developmental trajectory of the preterm-infant gut resistome deviates from that of the antibiotic-naïve near-term infants in prolonged carriage of some ARGs (for example, *oqxA*, *oqxB*, *catI*, *fosA5* and *cdeA*), near absence of others (for example, *abeM*) and a general increase in the normalized abundance of these genes in the gut across all of the timepoints (Fig. 3g). Overall, we found that the model only modestly predicted the chronological age of preterm infants ($R^2 = 0.62$; Fig. 3f), suggesting that distinct patterns of resistome development emerge on the basis of antibiotic treatment status and gestational age at birth.

Persistence of MDR Enterobacteriaceae in the preterm IGM

Whole-metagenome shotgun sequencing is a powerful method for describing high-level microbiota composition and function, but it is less-well equipped to elucidate strain-level variation. The gut has been established as an early reservoir of bacteria that cause late onset bloodstream infections in neonates⁵⁸ and is dominated by multidrug-resistant (MDR) Proteobacteria³³, but the extent to which these early colonizing strains persist in the IGM is poorly defined. We hypothesized that early-life hospitalization and antibiotic treatment in preterm infants might create a gastrointestinal niche for such Proteobacteria that is not relinquished after discharge from the NICU. To better understand the persistence of specific bacterial

Table 1 | Clinical characteristics of infant cohorts analysed in this study

	Preterm early antibiotic exposure only (n = 9)	Preterm early and subsequent antibiotic exposure (n = 32)	Term antibiotic-naïve infants (n = 17)
Birth weight (g), median (IQR)	1,080 (880, 1,270)	830 (698.75, 897.5)	2,529 (2,359.5, 2,966.5)
Gestational age (weeks) at birth median (IQR)	27 (26, 27)	25 (24, 26)	36 (36, 37)
Gender, male/female	4/5	15/17	4/13
Route of delivery, Caesarean section/vaginal	6/3	25/7	15/2
Antibiotic exposure, number of courses			
Gentamicin	9	74	None
Ampicillin	9	37	None
Vancomycin	None	67	None
Clindamycin	None	16	None
Meropenem	None	14	None
Cefepime	None	11	None
Cefotaxime	None	10	None
Mupirocin	None	7	None
Trimethoprim-sulfamethoxazole	None	4	None
Ticarcillin-clavulanate	None	3	None
Oxacillin	None	3	None
Cefoxitin	None	3	None
Cefazolin	None	2	None
Amoxicillin	None	2	None
Metronidazole	None	1	None
Penicillin G	None	1	None
Bacterial culture positive (n)			
Blood	0	22	0
Trachea	0	30	0
Urine	0	17	0

strains in the microbiota of infants in our cohort, we cultured pairs of stools collected 8–10 months apart from 15 infants (9 preterm and 6 near-term) on a series of selective agars (see Methods). We optimized culture conditions to isolate opportunistic extraintestinal pathogens that are known to be highly prevalent and are abundant in the IGM as well as those that are frequently MDR. In total, we cultured 530 isolates from these 30 samples. We whole-genome sequenced, assembled and annotated 277 and 253 isolates from the preterm and near-term sets, respectively.

The species most frequently isolated by this direct selection were *E. coli* ($n = 139$), *K. pneumoniae* ($n = 62$), *E. faecalis* ($n = 50$), *Enterobacter cloacae* ($n = 42$), *Enterococcus faecium* ($n = 22$), *Citrobacter freundii* ($n = 15$) and *Klebsiella oxytoca* ($n = 14$). We identified within-infant persistence of nearly identical strains of *E. coli*, *E. cloacae* and *K. variicola* in samples collected from both preterm and near-term infants. These highly similar, persistent isolate pairs from infants included isolates from samples collected both while in the hospital and after discharge (Fig. 4).

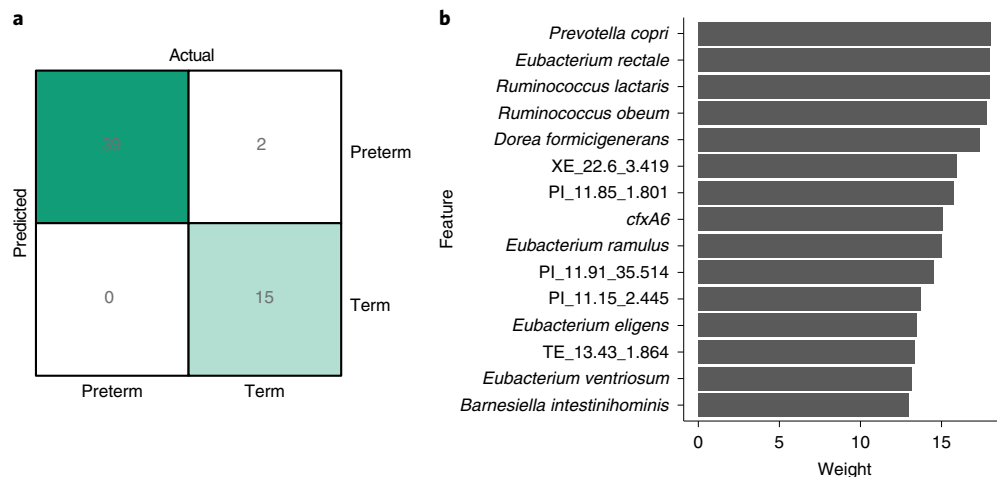


Fig. 5 | Enduring damage to the preterm IGM. a, Support vector machine confusion matrix for the classification of gestational age on the basis of the species and ARGs present in the microbiota following discharge from the NICU or at matched timepoints in unhospitalized near-term infants. **b**, The 15 predictors that are most important to classification. A sparse model trained using only these 15 predictors was highly accurate (96.4% classification accuracy), a persistent metagenomic signature of preterm birth and associated hospitalization and antibiotic treatment.

Among the persistent isolates recovered were strains of *E. coli* ST405 and *E. cloacae* ST108, both of which are high-risk lineages known to encode extended-spectrum β -lactamases and NDM-family carbapenemases^{59–61}. Each of the *E. coli* strains encoded a TEM-1 β -lactamase as well as an aac(3)-IId aminoglycoside acetyltransferase with predicted resistance to aminoglycosides, and each *E. cloacae* strain encoded an AmpC type β -lactamase. The *K. variicola* strains each contained *oqxAB*, which encodes the RND-type multidrug efflux pump⁶², and the chromosomal *Klebsiella* β -lactamase *blaOKP-B-1*⁶³ (Supplementary Table 4). We isolated nearly identical MDR Enterobacteriaceae—as suggested by the average nucleotide identity of more than 99.997% (Fig. 4b,d,f) and core gene single-nucleotide-polymorphism distances (Supplementary Table 4)—from the preterm IGM both in the NICU and after discharge. These data support an enduring and transmissible pathological microbiome scar associated with preterm birth, early-life hospitalization and antibiotic treatment.

As *Enterococcus* species are prevalent and abundant in the preterm-infant gut³³, often MDR⁶⁴, and cause nosocomial blood stream infections in preterm infants⁶⁵, we investigated their resistance and virulence phenotypes. A particular concern among hospitalized populations is vancomycin-resistant *Enterococci*⁶⁶. Of the 15 unique *Enterococcus* strains that we isolated, ten were *E. faecalis* and five were *E. faecium* (Supplementary Fig. 7a). No *E. faecalis*, and two *E. faecium* isolates were resistant to vancomycin. However, no *E. faecium* strain formed a biofilm, whereas four of the *E. faecalis* strains formed robust biofilms at room temperature and an additional six strains formed biofilms at 37 °C (Supplementary Fig. 7b). Interestingly, all of the biofilm-forming strains were isolated from preterm-infant stool. This is consistent with the prevailing understanding that early colonizers of the preterm-infant gut are largely surface-adapted strains that are prevalent in the NICU environment⁶⁷. The biofilm-forming strains of *E. faecalis*, although susceptible to vancomycin when planktonic, were resistant to this antibiotic when in biofilms (Supplementary Fig. 7c). Thus, despite the apparent trade-off between vancomycin resistance and biofilm formation observed among *Enterococcus* strains, nearly all have evolved strategies for surviving vancomycin treatment. This is concerning given the widespread usage of vancomycin (Table 1) and prevalence of *Enterococcus* colonization (Fig. 1b) in the NICU.

Persistent metagenomic signature of antibiotic treatment

To understand whether prematurity, hospitalization and antibiotic treatment had persistent effects on gut microbial content and function, we sought to identify metagenomic features that distinguished post-NICU discharge samples in preterm infants from age-matched samples from antibiotic-naïve near-term infants. We used a supervised learning approach to classify samples as originating from a hospitalized preterm infant (including both early-only and early-and-subsequent antibiotic treatment groups) or an antibiotic-naïve near-term infant residing at home, on the basis of the relative abundance of bacterial taxa and ARGs in their IGM. Using a support vector machine, we identified the 15 most informative features and constructed a model consisting of only these variables, which correctly classified all of the preterm and 15 of the 17 near-term samples (96.4% accuracy; Fig. 5a). Of the 15 variables that were most important to model performance, six were ARGs and nine were bacterial taxa (Fig. 5b). The ARGs important to classification were the class A β -lactamase *cfxA6*⁶⁸, and five genes functionally selected on piperacillin or tetracycline. The highest identity BLAST hit of four of the functionally selected ARGs was an ABC transporter, whereas the other was a MATE family efflux transporter. The predictive species were members of the order Clostridiales (*Eubacterium rectale*, *Ruminococcus obeum*, *Ruminococcus lactaris*, *Dorea formicigenerans*, *Eubacterium ventriosum*, *Eubacterium ramulus* and *Eubacterium eligens*) and Bacteroidales (*Prevotella copri* and *Barnesiella intestinihominis*). Our model accurately identified whether a preterm infant was hospitalized and received early-life antibiotic treatment on the basis of metagenome composition following NICU discharge despite high-level architectural recovery.

Conclusion

By combining metagenomic sequencing, selective and differential stool culture paired with isolate sequencing, functional metagenomics and machine learning, we demonstrate persistent metagenomic signatures of early-life antibiotic treatment and hospitalization in preterm infants. These signatures are characterized by an enriched gut resistome and persistent carriage of MDR Enterobacteriaceae, despite apparent recovery in microbiota maturity. Regardless of prematurity or antibiotic exposure, we observed little variation in the functional capacity of the microbiota, albeit using broad functional categories. Our work highlights the need to integrate sequencing- and culture-based

approaches for examining microbiota to reveal underappreciated effects of perturbations. These complementary methods provide data that support a persistent metagenomic signature of early-life hospitalization and antibiotic treatment associated with prematurity in the dynamic microbial community housed in the infant gut.

We were unable to isolate the effects of antibiotics from those of other adverse early-life events that coincide with prematurity, such as extended hospitalization and illness. Although an interventional study to probe these variables in neonates is infeasible, future animal studies could provide important insights into their relative contributions. Furthermore, it is probable that yet-to-be-defined environmental variables play a role in the co-development of the immune system and the microbiota, which needs to be addressed in future studies. Despite these caveats, we found compelling evidence for the underappreciated lasting effect of prematurity and the associated hospitalization and antibiotic treatment on the microbiome. These perturbations may play a role in chronic pathologies associated with prematurity for which the aetiology is unclear. From a clinical standpoint, our findings emphasize a necessity for alternatives to broad-spectrum antimicrobial therapy for managing infection in the NICU. This should not only entail therapeutic approaches, such as narrow-spectrum antibiotics and probiotic therapies⁶⁹, but also improved accuracy and speed of diagnostics to reduce unnecessary courses of antibiotics. It is unclear whether these results are generalizable across NICUs. Future multicentre studies are important to reveal the effect of neonatal antibiotic stewardship practices in IGM development. Although the metagenomic scars that we identified may be implicated in sequelae of preterm birth, such as neurodevelopmental^{70–72}, metabolic^{73,74}, cardiac^{75,76} and respiratory^{77,78} defects, further experiments with model systems, including gnotobiotic animals, are needed to link these enduring dysbioses and lasting pathologies.

Methods

Sample and metadata collection. All of the samples and patient metadata used in this study were collected as part of the Neonatal Microbiome and Necrotizing Enterocolitis Study (P.I.T. and B.B.W.) or the St Louis Neonatal Microbiome Initiative (B.B.W. and P.I.T.) at Washington University School of Medicine and approved by the Human Research Protection Office (approval numbers 201105492 and 201104267, respectively). Samples were obtained from infants after parents provided informed consent. As very few hospitalized preterm infants are antibiotic naive, we stratified our cohort for sample analysis by antibiotic exposure and gestational age at birth, with a subset of individuals who received early antibiotic exposure only ($n=9$) and no antibiotic exposure outside the first week of life, a subset of individuals with early and subsequent antibiotic exposure ($n=32$), and a subset of late-preterm or early-term infants ($n=17$) who were not hospitalized and were antibiotic-naïve throughout the first months of life (Table 1). All of the stools produced were collected and stored as previously described^{79,80}. In total, 437 samples collected longitudinally from 58 infants were shotgun sequenced and included in all metagenomic analyses.

Metagenomic DNA extraction. Metagenomic DNA was extracted from approximately 100 mg of stool samples using the PowerSoil DNA Isolation Kit (MoBio Laboratories) following the manufacturer's protocol with the following modification: samples were lysed by two rounds of 2 min of bead beating at 2,500 oscillations min⁻¹ for 2 min followed by 1 min on ice and an additional 2 min of beadbeating using a Mini-Beadbeater-24 (Biospec Products). DNA was quantified using a Qubit fluorometer dsDNA HS Assay (Invitrogen) and stored at -20°C .

Preparation of the metagenomic sequencing library. Metagenomic DNA was diluted to a concentration of 0.5 ng μl^{-1} before preparation of the sequencing library. Libraries were prepared using a Nextera DNA Library Prep Kit (Illumina) following the modifications described previously by Baym et al.⁸¹. The libraries were purified using the Agencourt AMPure XP system (Beckman Coulter) and quantified using a Quant-iT PicoGreen dsDNA assay (Invitrogen). For each sequencing lane, 10 nM of approximately 96 samples was pooled three independent times. These pools were quantified using the Qubit dsDNA HS Assay and combined in an equimolar manner. Samples were then submitted for 2 × 150 bp paired-end sequencing on an Illumina NextSeq High-Output platform at the Center for Genome Sciences and Systems Biology at Washington University in St Louis with a target sequencing depth of 2.5 million reads per sample.

Rarefaction analysis. To determine the appropriate sequencing depth necessary to fully characterize IGM composition and function, 17 representative metagenomes

that were sequenced most deeply were subsampled at the following read depths: 8,000,000, 7,000,000, 6,000,000, 5,000,000, 4,000,000, 3,000,000, 2,000,000, 1,000,000, 100,000 and 10,000. Subsampled metagenomes were profiled using MetaPhlAn v.2.0⁴¹ to determine species richness at each depth. Rarefaction was only used to establish an appropriate sequencing depth, and subsampled metagenomes were not used for any downstream analyses.

Metagenome profiling. Before all downstream analyses, Illumina paired-end reads were binned by index sequence. Adapter and index sequences were trimmed and sequences were quality-filtered with Trimmomatic v.0.36⁶² using the following parameters: java -Xms2048m -Xmx2048m -jar trimmomatic-0.33.jar PE -phred33 ILLUMINACLIP:NexteraPE-PE.fa:2:30:10:1:true SLIDINGWINDOW:6:10 LEADING:13 TRAILING:13 MINLEN:36. Relative abundance of species was calculated using MetaPhlAn v.2.0⁴¹ (repository tag 2.2.0). Relative abundance tables were merged using the 'merge_metaphlan_tables.py' script. Abundance of metabolic pathways was determined using HUMAnN2⁴². Raw count values were normalized for sequencing depth, collapsed by ontology and tables were merged using the 'humann2_renorm_table', 'humann2_regroup_table' and 'humann2_join_tables' utility scripts.

Construction of metagenomic libraries from infant gut samples for functional selection. We constructed 22 functional metagenomic libraries by pooling metagenomic DNA from 9–10 stools per library, encompassing 396 Gb of metagenomic DNA with an average library size of 18 Gb (Supplementary Fig. 4, Supplementary Table 1) and an average insert size of 2–3 kb. Approximately 5 μg purified extracted total metagenomic DNA was used as starting material for the metagenomic library construction. To create small-insert metagenomic libraries, DNA was sheared to a target size of 3,000 bp using the Covaris E210 sonicator following the manufacturer's recommended settings (http://covarisinc.com/wp-content/uploads/pn_400069.pdf). Sheared DNA was then concentrated using a QIAquick PCR Purification Kit (Qiagen) and then eluted in 30 μl nuclease-free H₂O. The purified DNA was then size-selected using a BluePippin instrument (Sage Science) to a range of 1,000–6,000 bp fragment through a premade 0.75% Pippin gel cassette. Size-selected DNA was then end-repaired using an End-It DNA End Repair kit (Epicentre) with the following protocol:

- (1) Mix the following in a 50 μl reaction volume: 30 μl of purified DNA, 5 μl dNTP mix (2.5 mM), 5 μl 10× End-Repair buffer, 1 μl End-Repair Enzyme Mix and 4 μl nuclease-free H₂O.
- (2) Mix gently and incubate at room temperature for 45 min.
- (3) Heat inactivate the reaction at 70 $^{\circ}\text{C}$ for 15 min.

End-repaired DNA was then purified using the QIAquick PCR purification kit (Qiagen) and quantified using the Qubit fluorometer HS assay kit (Life Technologies) and ligated into a pZE21-MCS-1 vector at the HincII site. The pZE21 vector was linearized at the HincII site using inverse PCR with PFX DNA polymerase (Life Technologies):

- (1) Mix the following in a 50 μl reaction volume: 10 μl of 10× PFX reaction buffer, 1.5 μl of 10 mM dNTP mix (New England BioLabs), 1 μl of 50 mM MgSO₄, 5 μl of PFX enhancer solution, 1 μl of 100 pg μl^{-1} 21 circular pZE21, 0.4 μl of PFX DNA polymerase, 0.75 μl forward primer (5'-GACGGTATCGATAA-GCTTGAT-3'), 0.75 μl reverse primer (5'-GACCTCGAGGGGGG-3') and 29.6 μl of nuclease-free H₂O, to a final volume of 50 μl .
- (2) PCR cycle temperature as follows: 95 $^{\circ}\text{C}$ for 5 min, then 35 cycles of (95 $^{\circ}\text{C}$ for 45 s, 55 $^{\circ}\text{C}$ for 45 s, 72 $^{\circ}\text{C}$ for 2.5 min), then 72 $^{\circ}\text{C}$ for 5 min.

Linearized pZE21 was size-selected (~2,200 bp) on a 1% low melting point agarose gel (0.5× TBE) stained with GelGreen dye (Biotium) and purified by QIAquick Gel Extraction Kit (Qiagen). Pure vector was dephosphorylated using calf-intestinal alkaline phosphatase (CIP, New England BioLabs) by adding 1/10 reaction volume of CIP, 1/10 reaction volume of New England BioLabs Buffer 3 and nuclease-free H₂O to the vector eluate, and incubating at 37 $^{\circ}\text{C}$ overnight before heat inactivation for 15 min at 70 $^{\circ}\text{C}$. End-repaired metagenomic DNA and the linearized vector were ligated together using the Fast-Link Ligation Kit (Epicentre) at a 5:1 ratio of insert:vector using the following protocol:

- (1) Mix the following in a 15 μl reaction volume: 1.5 μl 10× Fast-Link buffer, 0.75 μl ATP (10 mM), 1 μl FastLink DNA ligase (2 U μl^{-1}), 5:1 ratio of metagenomic DNA:vector and nuclease-free H₂O to final reaction volume.
- (2) Incubate at room temperature overnight.
- (3) Heat inactivate for 15 min at 70 $^{\circ}\text{C}$.

After heat inactivation, ligation reactions were dialysed for 30 min using a 0.025 μm pore-size cellulose membrane (Millipore, VSWP09025) and the full reaction volume was used for transformation by electroporation into 25 μl *E. coli* MegaX (Invitrogen) according to the manufacturer's recommended protocols (http://tools.invitrogen.com/content/sfs/manuals/megax_man.pdf). Cells were recovered in 1 ml Recovery Medium (Invitrogen) at 37 $^{\circ}\text{C}$ for 1 h. Libraries were titred by plating onto 0.1 μl and 0.01 μl of recovered cells onto Luria-Bertani (LB) agar plates containing 50 $\mu\text{g ml}^{-1}$ kanamycin. For each library, the insert size distribution was estimated by gel electrophoresis of PCR products obtained by

amplifying the insert from 36 randomly picked clones using primers flanking the HincII site of the multiple cloning site of the pZE21-MCS1 vector (which contains a selectable marker for kanamycin resistance). The average insert size across all libraries was determined to be 3 kb, and library size estimates were calculated by multiplying the average PCR-based insert size by the number of titred colony-forming units (CFUs) after transformation recovery. The rest of the recovered cells were inoculated into 50 ml of LB containing 50 µg ml⁻¹ kanamycin and grown overnight. The overnight culture was frozen with 15% glycerol and stored at -80°C for subsequent screening.

Functional selections for antibiotic resistance. Each metagenomic library was selected for resistance to each of 16 antibiotics (at the concentrations listed in Supplementary Table 3 supplemented with 50 µg ml⁻¹ kanamycin for plasmid library maintenance) was performed using LB agar. Of note, as our library host—*E. coli*—is intrinsically resistant to vancomycin, we are unable to functionally screen for loci conferring resistance to this antibiotic. Furthermore, the use of kanamycin as the selective marker for the metagenomic plasmid library results in low-level cross-resistance with other aminoglycoside antibiotics, resulting in a higher required minimum inhibitory concentration for gentamicin. For each metagenomic library, the number of cells plated on each antibiotic selection represented 10× the number of unique CFUs in the library, as determined by titres during library creation. Depending on the titre of live cells following library amplification and storage, the appropriate volume of freezer stocks were either diluted to 100 µl using MH broth + 50 µg ml⁻¹ kanamycin or centrifuged and reconstituted in this volume for plating. After plating (using sterile glass beads), antibiotic selections were incubated at 37°C for 18 h to enable the growth of clones containing an antibiotic-resistance-conferring DNA insert. Of the 352 antibiotic selections performed, 296 yielded antibiotic-resistant *E. coli* transformants (Supplementary Fig. 4). After overnight growth, all of the colonies from a single antibiotic plate (library by antibiotic selection) were collected by adding 750 µl of 15% LB-glycerol to the plate and scraping with an L-shaped cell scraper to gently remove colonies from the agar. The slurry was then collected and this process was repeated a second time for a total volume of 1.5 ml to ensure that all of the colonies were removed from the plate. The bacterial cells were then stored at -80°C before PCR amplification of antibiotic-resistant metagenomic fragments and Illumina library creation.

Amplification and sequencing of functionally selected fragments. Freezer stocks of antibiotic-resistant transformants were thawed and 300 µl of cells were pelleted by centrifugation at 13,000 r.p.m. for 2 min and then gently washed with 1 ml of nuclease-free H₂O. Cells were subsequently pelleted a second time and resuspended in 30 µl of nuclease-free H₂O. Resuspensions were then frozen at -20°C for 1 h and thawed to promote cell lysis. The thawed resuspension was pelleted by centrifugation at 13,000 r.p.m. for 2 min and the resulting supernatant was used as template for amplification of resistance-conferring DNA fragments by PCR using Taq DNA polymerase (New England BioLabs):

- (1) Mix the following for a 25 µl reaction volume: 2.5 µl of DNA template, 2.5 µl of ThermoPol reaction buffer (New England BioLabs), 0.5 µl of 10 mM deoxynucleotide triphosphates (dNTPs, New England BioLabs), 0.5 µl of Taq polymerase (5 U µl⁻¹), 3 µl of a custom primer mix and 16 µl of nuclease-free H₂O.
- (2) PCR cycle temperatures were as follows: 94°C for 10 min, then 25 cycles of (94°C for 45 s, 55°C for 45 s, 72°C for 5.5 min) and finally 72°C for 10 min.

The custom primer mix consisted of three forward and three reverse primers, each targeting the sequence immediately flanking the HincII site in the pZE21-MCS1 vector, and staggered by one base pair. The staggered primer mix ensured a diverse nucleotide composition during early Illumina sequencing cycles and contained the following primer volumes (from a 10 mM stock) in a single PCR reaction: primer F1, CCGAATTCATTAAAGAGGAGAAAG, 0.5 µl; primer F2, CGAATT CATTAAAGAGGAGAAAGG, 0.5 µl; primer F3, GAATTCATTAAAGAGGAGAAAGGTAC, 0.5 µl; primer R1, GATATCAAGCTTATCGATACCGTC, 0.21 µl; primer R2, CGATATCAAGCTTATCGATACCG, 0.43 µl; and primer R3, TCGATATCAAGCTTATCGATACCG, 0.86 µl. The amplified metagenomic inserts were then cleaned using the Qiagen QIAquick PCR purification kit and quantified using the Qubit fluorometer HS assay kit (Life Technologies).

For amplified metagenomic inserts from each antibiotic selection, elution buffer was added to the PCR template for a final volume of 200 µl and sonicated in a half-skirted 96-well plate using a Covaris E210 sonicator with the following setting: duty cycle, 10%; intensity, 5; cycles per burst, 200; sonication time, 600 s. After sonication, sheared DNA was purified and concentrated using the MinElute PCR Purification kit (Qiagen) and eluted in 20 µl of prewarmed nuclease-free H₂O. In the first step of library preparation, purified sheared DNA was end-repaired:

- (1) Mix the following for a 25 µl reaction volume: 20 µl of elute, 2.5 µl T4 DNA ligase buffer with 10 mM ATP (10×, New England BioLabs), 1 µl dNTPs (1 mM, New England BioLabs), 0.5 µl T4 polymerase (3 U µl⁻¹, New England BioLabs), 0.5 µl T4 PNK (10 U µl⁻¹, New England BioLabs) and 0.5 µl Taq Polymerase (5 U µl⁻¹, New England BioLabs).

- (2) Incubate the reaction at 25°C for 30 min followed by 20 min at 75°C.

Next, 5 µl of 1 µM pre-annealed, barcoded sequencing adapters were added to each end-repaired sample (adapters were thawed on ice). Barcoded adapters consisted of a unique 7-bp oligonucleotide sequence specific to each antibiotic selection, facilitating the demultiplexing of mixed-sample sequencing runs. Forward and reverse sequencing adapters were stored in TES buffer (10 mM Tris, 1 mM EDTA, 50 mM NaCl, pH 8.0) and annealed by heating the 1 µM mixture to 95°C followed by a slow cool (0.1°C s⁻¹) to a final holding temperature of 4°C. After the addition of barcoded adapters, samples were incubated at 16°C for 40 min and then for 10 min at 65°C. Before size selection, 10 µl each of adapter-ligated samples were combined into pools of 12 and concentrated by elution through a MinElute PCR Purification Kit (Qiagen), eluting in 14 µl of elution buffer (10 mM Tris-Cl, pH 8.5). The pooled, adapter-ligated, sheared DNA was then size-selected to a target range of 300–400 bp on a 2% agarose gel in 0.5× TBE, stained with GelGreen dye (Biotium) and extracted using a MinElute Gel Extraction Kit (Qiagen). The purified DNA was enriched using the following protocol:

- (1) Mix the following for a 25 µl reaction volume: 2 µl of purified DNA, 12.5 µl 2× Phusion HF Master Mix (New England BioLabs), 1 µl of 10 mM Illumina PCR Primer Mix (5'-AATGATACGGCGACCACCGAGATC-3' and 5'-CAAGCAGAAGACGGCATACGAGAT-3'), and 9.5 µl of nuclease-free H₂O.
- (2) The PCR cycle was as follows: 98°C for 30 s, then 18 cycles of (98°C for 10 s, 65°C for 30 s, 72°C for 30 s) and then 72°C for 5 min.

Amplified DNA was measured using the Qubit fluorometer HS assay kit (Life Technologies) and 10 nM of each sample was pooled for sequencing. Subsequently, samples were submitted for paired-end 101 bp sequencing using an Illumina Next Seq platform at the DNA Sequencing and Innovation Laboratory at the Edison Center for Genome Sciences and Systems Biology, Washington University in St Louis. In total, three sequence runs were performed at a concentration of 10 pM per lane.

Assembly and annotation of functionally selected fragments. Illumina paired-end sequence reads were binned by barcode (exact match required) such that independent selections were assembled and annotated in parallel. Assembly of the resistance-conferring DNA fragments from each selection was achieved using PARFuMS⁴⁹ (Parallel Annotation and Reassembly of Functional Metagenomic Selections), a tool developed specifically for the high-throughput assembly and annotation of functional metagenomic selections.

ORFs were predicted in assembled contigs using MetaGeneMark⁸³ and annotated by searching amino acid sequences against Pfam, TIGRFAMs and an ARG-specific profile hidden-Markov-model (pHMM) database, Resfams⁸⁴ (<http://www.dantaslab.org/resfams>), using HMMER3⁸⁵. MetaGeneMark was run using default gene-finding parameters and 'hmmsearch' (HMMER3) was run with the option --cut_ga as implemented in the script 'annotate_functional_selections.py'. Selections were excluded from analysis if (1) more than 200 contigs were assembled or (2) the number of contigs assembled exceeded the number of colonies on the selection plate by a factor of ten. Furthermore, assembled contigs of less than 500 bp were discarded. As many assembled contigs include multiple annotated ORFs, the subset of proteins that are considered to be causative resistance determinants for downstream analysis were classified using the following hierarchical scheme. First, if a contig encoded a protein with a 100% amino acid identity hit to the CARD database³¹, it was considered to be the causative resistance determinant on that contig. Next, if a contig encoded a protein with a significant hit to a Resfams pHMM using profile-specific gathering thresholds, it was considered to be the causative resistance determinant on that contig. In the absence of a high-scoring hit to the CARD or Resfams databases, contigs were manually curated to identify plausible resistance determinants on an antibiotic-specific basis. The rationale for this hierarchical classification scheme was to first identify perfect matches to known resistance determinants through BLAST to CARD (with a threshold of 100% amino acid identity), and subsequently identify variants of known resistance determinants using Resfams pHMMs. Using these criteria, 1,184 of the 5,658 unique predicted proteins (20.9%) were classified as resistance determinants.

The percentage identity of all resistance determinants were determined using BLASTp⁸⁶ queries against both the NCBI non-redundant protein database (retrieved 21 May 2018) and the CARD³¹ database (v.1.2.1, retrieved 24 January 2018). Once the top local alignment was identified using BLASTp, it was used for a global alignment using the Needleman–Wunsch algorithm as implemented in the 'needle' program of EMBOSS⁸⁷ v.6.6.0 as previously described³³.

Putative mobile genetic elements were identified on functionally selected contigs on the basis of string matches to one of the following keywords in Pfam and TIGRFAMs annotations: 'transposase', 'transposon', 'conjugative', 'integrase', 'integron', 'recombinase', 'conjugal', 'mobilization', 'recombination' or 'plasmid'.

Quantification of ARGs in metagenomes. The relative abundance of ARGs was calculated using ShortBRED³⁰. Causative resistance determinants, as identified using the hierarchical annotation scheme described above, were used as proteins of interest for the identification of marker families using 'shortbred_identify.py'. These proteins included all of the ARGs in CARD (v.1.2.1, retrieved 24 January 2018)³¹ and

antibiotic-resistance proteins identified using functional metagenomic selections performed in the current study. Thus, the custom ShortBRED database included markers to canonical antibiotic-resistance determinants as well as resistance determinants functionally identified in this study that are most relevant to the IGM. To calculate the relative abundance of resistance genes in metagenomes, 'shortbred_quantify.py' was used.

Bacterial isolation from infant stools. Approximately 50 mg of frozen stool was resuspended in 1 ml tryptic soy broth (TSB) and incubated with shaking at 37 °C for 4 h. Then, 50 µl of culture was streaked for isolation using the four-quadrant method on each of the following agars: bile esculin agar, ESB agar, MacConkey agar, MacConkey agar + cefotaxime, MacConkey agar + ciprofloxacin, and blood agar (Hardy Diagnostics, G12, G321, G35, G121, G258 and A10, respectively). The plates were incubated for 18–24 h at 37 °C. Four colonies of each distinct morphology on each plate were sub-streaked onto blood agar and incubated for 18–24 h at 37 °C. Following confirmation of morphology, a 1 ml TSB was inoculated with a single colony and grown overnight at 37 °C with shaking. Overnight cultures were frozen in 15% glycerol in TSB.

Isolation of genomic DNA. For the isolation of genomic DNA, 1.5 ml TSB was inoculated from isolate glycerol stocks and grown overnight at 37 °C with shaking. DNA was extracted using the BioStic Bacteremia DNA Isolation Kit (MoBio Laboratories) following the manufacturer's protocols. Genomic DNA was quantified using a Qubit fluorometer dsDNA HS Assay (Invitrogen) and stored at –20 °C.

Preparation of the isolate sequencing libraries. Isolate sequencing libraries were prepared in the same manner as described for metagenomic sequencing libraries, following the protocol described previously by Baym et al.⁸¹ For each sequencing lane, 10 nM of approximately 300 samples were pooled three independent times. These pools were quantified using the Qubit dsDNA HS Assay and combined in an equimolar manner. Samples were then submitted for 2 × 150 bp paired-end sequencing on an Illumina NextSeq High-Output platform at the Center for Genome Sciences and Systems Biology at Washington University in St Louis with a target sequencing depth of 1 million paired-end reads per sample.

Assembly of isolate genomes. Before all downstream analyses, Illumina paired-end reads were binned by index sequence. Adapter and index sequences were trimmed using Trimmomatic v.0.36⁸² using the following parameters: java -Xms2048m -Xmx2048m -jar trimmomatic-0.33.jar PE -phred33 ILLUMINACLIP: NexteraPE-PE.fa:2:30:10:1:true. Contaminating human reads were removed using DeconSeq⁸⁸ and unpaired reads were discarded. Reads were assembled with SPAdes⁸⁹ using the following parameters: spades.py -k 21,33,55,77 -careful. Contigs that were less than 500 bp were excluded from further analysis. Assembly quality was assessed using QUAST⁹⁰. Average coverage across the assembly was calculated by mapping raw reads to contigs using bbmap (<https://jgi.doe.gov/data-and-tools/bbtools/>).

Genomic analysis of isolates. A total of 406 assemblies had an N50 of greater than 50,000 bp and fewer than 500 total contigs longer than 1,000 bp and were included in further analysis. Genomes were annotated using Prokka⁹¹ with default parameters. Multilocus sequence types were determined using in silico MLST (<https://github.com/tseemann/mlst>). Species assignments were determined by querying assemblies against a RefSeq sketch using Mash identifying RefSeq hits with the minimum Mash distance⁹². Assemblies were binned by species according to Mash designation. For each of the seven most commonly occurring species, pangenome analysis was performed using Roary, with core-genome alignments created using PRANK⁹³. An outgroup assembly of the same genus but different species was downloaded from NCBI and included in each pangenome analysis (Supplementary Table 2). Maximum-likelihood core-genome phylogenies were constructed using RAXML under the GTRGAMMA model with 1,000 bootstraps and maximum-likelihood optimization initialized from a random starting tree. Average nucleotide identities were computed using pyani (<https://github.com/widowquinn/pyani>). Pairwise single-nucleotide polymorphism distances were calculated from core-genome alignments generated by Roary using snp-dists (<https://github.com/tseemann/snp-dists>). Resistance genes were annotated by nucleotide BLAST to the ResFinder database (<https://bitbucket.org/genomicepidemiology/resfinder/src/master/README.md>).

Enterococcus biofilm formation assay. Mid-log phase cultures in freshly prepared tryptic soy broth containing 0.5% glucose (TSBG) were diluted to an optical density of 0.1 at 600 nm. Then, 200 µl of the diluted culture was added in quadruplicate to 96-well polystyrene plates and incubated at room temperature or 37 °C without shaking. After 24 h of growth, wells were decanted, washed three times with sterile PBS and fixed for 30 min with 200 µl Bouin's solution. Fixative was removed by washing three times with sterile PBS, then wells were stained with 0.1% crystal violet for 30 min. Excess stain was removed by washing three times with sterile PBS, the stain was solubilized in 200 µl ethanol and absorbance was read at 590 nm. The *E. faecalis* strains TX5682 (biofilm negative) and TX82 (biofilm positive) were used as controls⁹⁴.

Enterococcus vancomycin susceptibility testing. Isolates identified as *Enterococcus* were phenotyped for vancomycin resistance using microbroth dilution according to the CLSI guidelines. ATCC29212 (vancomycin-susceptible) and ATCC51299 (vancomycin-resistant) were included in all of the assays as controls. Isolates were grown to mid-log phase, diluted in culture media to 1 × 10⁶ CFU ml⁻¹ and used to inoculate plates containing vancomycin at a concentration ranging from 128 to 2 µg ml⁻¹. After 24 h of static growth at 37 °C, optical density was read at 600 nm and the minimum inhibitory concentration was determined by scoring by eye for turbidity.

Vancomycin resistance of biofilms was assayed after establishing biofilms as above. After 24 h of static growth at 37 °C, planktonic cells were removed by washing three times with sterile water and then with 200 µl of TSBG containing 5 mg ml⁻¹, 5 µg ml⁻¹ or no vancomycin, and the plates incubated at 37 °C for an additional 24 h. After washing planktonic cells three times with sterile water, 200 µl sterile water was added to each well and the viability of the cells in the biofilm was assessed using an XTT Cell Viability Kit (Cell Signaling Technology, 9095) according to the manufacturer's protocols, reading absorbance at 450 nm 60 min after the addition of reagents.

Generalized linear mixed model of microbiota diversity. To model the effect of clinical variables on microbiota diversity, a generalized linear mixed model was fit by maximum likelihood using the lme4 package in R. All of the variables in Supplementary Table 1 were included in initial modelling, and a final model was fit by backwards elimination of variables. Pseudo-R² was determined using the 'rsquaredGLMM' function in the 'MuMIn' package. *P* values were corrected for multiple hypotheses using the glht function in the multcomp (lincf = mcp(tension = 'Tukey')).

Prediction of microbiota age using random forests. Random forest models were used to regress the relative abundances of all of the species predicted by MetaPhlAn2 in infant stool samples against their chronological age using the R package 'randomForest' as previously described⁴⁸. The default parameters were used with the following exceptions: ntree = 10,000, importance = TRUE. Fivefold cross-validation was performed using the 'rfcv' function over 100 iterations to estimate the minimum number of features needed to accurately predict microbiota age. The features most important for prediction were identified over 100 iterations of the 'importance' function, and a sparse model consisting of the 50 most important features was constructed and trained on a set of nine antibiotic-naïve near-term infants randomly selected from the larger near-term infant set. This model was validated in the remaining eight antibiotic-naïve near-term infants, and then applied to preterm infants to predict microbiota age. The MAZ was computed as previously described⁴⁸. This enabled comparisons of microbiota maturity between age bins as the metric accounts for differing variance in predicted microbiota age throughout infant development.

Classification of post-discharge samples. A single sample from each individual was selected (the final post-discharge sample collected from each preterm infant and a roughly age-matched sample from each near-term infant). All metagenomic data (species and ARG abundances, centred and scaled) were initially used as input for logistic regression, *k*-nearest neighbour, support vector machine, naïve Bayes and random forests classifiers. Ultimately, a support vector machine as implemented in the R package e1071 was selected as it was both the highest performing and the most parsimonious classifier. Feature importance was determined by computing the element-wise absolute value of the matrix of weights by the matrix of support vectors. A sparse model was subsequently constructed consisting of only the 15 most important features.

Reporting Summary. Further information on research design is available in the Nature Research Reporting Summary linked to this article.

Data availability

Assembled functional metagenomic contigs, shotgun metagenomic reads, shotgun genomic reads and assemblies have been deposited to NCBI GenBank and SRA under BioProject ID PRJNA489090.

Code availability

The software packages used in this study are free and open source. Analysis scripts used here (and associated usage notes) are available from the authors on reasonable request.

Received: 28 September 2018; Accepted: 26 July 2019;

Published online: 09 September 2019

References

- Sommer, F. & Bäckhed, F. The gut microbiota—masters of host development and physiology. *Nat. Rev. Microbiol.* **11**, 227–238 (2013).
- Pantoja-Feliciano, I. G. et al. Biphasic assembly of the murine intestinal microbiota during early development. *ISME J.* **7**, 1112–1115 (2013).

3. Yatsunenkov, T. et al. Human gut microbiome viewed across age and geography. *Nature* **486**, 222–227 (2012).
4. Cox, L. M. et al. Altering the intestinal microbiota during a critical developmental window has lasting metabolic consequences. *Cell* **158**, 705–721 (2014).
5. Abrahamsson, T. R. et al. Low gut microbiota diversity in early infancy precedes asthma at school age. *Clin. Exp. Allergy* **44**, 842–850 (2014).
6. Livanos, A. E. et al. Antibiotic-mediated gut microbiome perturbation accelerates development of type 1 diabetes in mice. *Nat. Microbiol.* **1**, 16140 (2016).
7. Cho, I. et al. Antibiotics in early life alter the murine colonic microbiome and adiposity. *Nature* **488**, 621–626 (2012).
8. Lozupone, C. A., Stombaugh, J. I., Gordon, J. I., Jansson, J. K. & Knight, R. Diversity, stability and resilience of the human gut microbiota. *Nature* **489**, 220–230 (2012).
9. Trasande, L. et al. Infant antibiotic exposures and early-life body mass. *Int. J. Obes.* **37**, 16–23 (2013).
10. Hviid, A., Svanstrom, H. & Frisch, M. Antibiotic use and inflammatory bowel diseases in childhood. *Gut* **60**, 49–54 (2011).
11. Penders, J. et al. Gut microbiota composition and development of atopic manifestations in infancy: the KOALA birth cohort study. *Gut* **56**, 661–667 (2007).
12. Arrieta, M.-C. et al. Early infancy microbial and metabolic alterations affect risk of childhood asthma. *Sci. Transl. Med.* **7**, 307ra152 (2015).
13. Ahmadizar, F. et al. Early life antibiotic use and the risk of asthma and asthma exacerbations in children. *Pediatr. Allergy Immunol.* **28**, 430–437 (2017).
14. Stokholm, J. et al. Maturation of the gut microbiome and risk of asthma in childhood. *Nat. Commun.* **9**, 141 (2018).
15. Missaghi, B., Barkema, H., Madsen, K. & Ghosh, S. Perturbation of the human microbiome as a contributor to inflammatory bowel disease. *Pathogens* **3**, 510–527 (2014).
16. Tremlett, H. et al. Gut microbiota in early pediatric multiple sclerosis: a case–control study. *Eur. J. Neurol.* **23**, 1308–1321 (2016).
17. Russell, S. L. et al. Early life antibiotic-driven changes in microbiota enhance susceptibility to allergic asthma. *EMBO Rep.* **13**, 440–447 (2012).
18. Zanvit, P. et al. Antibiotics in neonatal life increase murine susceptibility to experimental psoriasis. *Nat. Commun.* **6**, 8424 (2015).
19. Azad, M. B., Bridgman, S. L., Becker, A. B. & Kozyrskyj, A. L. Infant antibiotic exposure and the development of childhood overweight and central adiposity. *Int. J. Obes.* **38**, 1290–1298 (2014).
20. Boursi, B., Mamtani, R., Haynes, K. & Yang, Y.-X. The effect of past antibiotic exposure on diabetes risk. *Eur. J. Endocrinol.* **172**, 639–648 (2015).
21. Shaw, S. Y., Blanchard, J. F. & Bernstein, C. N. Association between the use of antibiotics in the first year of life and pediatric inflammatory bowel disease. *Am. J. Gastroenterol.* **105**, 2687–2692 (2010).
22. Ungaro, R. et al. Antibiotics associated with increased risk of new-onset Crohn's disease but not ulcerative colitis: a meta-analysis. *Am. J. Gastroenterol.* **109**, 1728–1738 (2014).
23. Kronman, M. P., Zaoutis, T. E., Haynes, K., Feng, R. & Coffin, S. E. Antibiotic exposure and IBD development among children: a population-based cohort study. *Pediatrics* **130**, e794–e803 (2012).
24. Lexmond, W. S. et al. Involvement of the iNKT cell pathway is associated with early-onset eosinophilic esophagitis and response to allergen avoidance therapy. *Am. J. Gastroenterol.* **109**, 646–657 (2014).
25. Blencowe, H. et al. National, regional, and worldwide estimates of preterm birth rates in the year 2010 with time trends since 1990 for selected countries: a systematic analysis and implications. *Lancet* **379**, 2162–2172 (2012).
26. Liu, L. et al. Global, regional, and national causes of under-5 mortality in 2000–15: an updated systematic analysis with implications for the sustainable development goals. *Lancet* **388**, 3027–3035 (2016).
27. Stoll, B. J. Neurodevelopmental and growth impairment among extremely low-birth-weight infants with neonatal infection. *JAMA* **292**, 2357 (2004).
28. Flannery, D. D. et al. Temporal trends and center variation in early antibiotic use among premature infants. *JAMA Netw. Open* **1**, e180164 (2018).
29. Rose, G. et al. Antibiotic resistance potential of the healthy preterm infant gut microbiome. *PeerJ* **5**, e2928 (2017).
30. Rahman, S. F., Olm, M. R., Morowitz, M. J. & Banfield, J. F. Machine learning leveraging genomes from metagenomes identifies influential antibiotic resistance genes in the infant gut microbiome. *mSystems* **3**, e00123-17 (2018).
31. Pärnänen, K. et al. Maternal gut and breast milk microbiota affect infant gut antibiotic resistome and mobile genetic elements. *Nat. Commun.* **9**, 3891 (2018).
32. Hourigan, S. K. et al. Comparison of infant gut and skin microbiota, resistome and virulome between neonatal intensive care unit (NICU) environments. *Front. Microbiol.* **9**, 1361 (2018).
33. Gibson, M. K. et al. Developmental dynamics of the preterm infant gut microbiota and antibiotic resistome. *Nat. Microbiol.* **1**, 16024 (2016).
34. Fouhy, F. et al. High-throughput sequencing reveals the incomplete, short-term recovery of infant gut microbiota following parenteral antibiotic treatment with ampicillin and gentamicin. *Antimicrob. Agents Chemother.* **56**, 5811–5820 (2012).
35. Greenwood, C. et al. Early empiric antibiotic use in preterm infants is associated with lower bacterial diversity and higher relative abundance of enterobacter. *J. Pediatr.* **165**, 23–29 (2014).
36. Stewart, C. J. et al. Preterm gut microbiota and metabolome following discharge from intensive care. *Sci. Rep.* **5**, 17141 (2015).
37. Zwiitink, R. D. et al. Association between duration of intravenous antibiotic administration and early-life microbiota development in late-preterm infants. *Eur. J. Clin. Microbiol. Infect. Dis.* **37**, 475–483 (2018).
38. Moles, L. et al. Preterm infant gut colonization in the neonatal ICU and complete restoration 2 years later. *Clin. Microbiol. Infect.* **21**, 936–936 (2015).
39. The American College of Obstetricians and Gynecologists Committee on Obstetric Practice Society for Maternal-Fetal Medicine Committee opinion No 579: Definition of term pregnancy. *Obstet. Gynecol.* **122**, 1139–1140 (2013).
40. Raju, T. N. K., Higgins, R. D., Stark, A. R. & Leveno, K. J. Optimizing care and outcome for late-preterm (near-term) infants: a summary of the workshop sponsored by the national institute of child health and human development. *Pediatrics* **118**, 1207–1214 (2006).
41. Truong, D. T. et al. MetaPhlAn2 for enhanced metagenomic taxonomic profiling. *Nat. Methods* **12**, 902–903 (2015).
42. Franzosa, E. A. et al. Species-level functional profiling of metagenomes and metatranscriptomes. *Nat. Methods* **15**, 962–968 (2018).
43. Bradley, P. H. & Pollard, K. S. Proteobacteria explain significant functional variability in the human gut microbiome. *Microbiome* **5**, 36 (2017).
44. Lindberg, T. P. et al. Preterm infant gut microbial patterns related to the development of necrotizing enterocolitis. *J. Matern. Fetal Neonatal Med.* **18**, 1–10 (2018).
45. Warner, B. B. et al. Gut bacteria dysbiosis and necrotising enterocolitis in very low birthweight infants: a prospective case-control study. *Lancet* **387**, 1928–1936 (2016).
46. Abrahamsson, T. R. et al. Low diversity of the gut microbiota in infants with atopic eczema. *J. Allergy Clin. Immunol.* **129**, 434–440 (2012).
47. Kriss, M., Hazleton, K. Z., Nusbacher, N. M., Martin, C. G. & Lozupone, C. A. Low diversity gut microbiota dysbiosis: drivers, functional implications and recovery. *Curr. Opin. Microbiol.* **44**, 34–40 (2018).
48. Subramanian, S. et al. Persistent gut microbiota immaturity in malnourished Bangladeshi children. *Nature* **510**, 417–421 (2014).
49. Forsberg, K. J. et al. The shared antibiotic resistome of soil bacteria and human pathogens. *Science* **337**, 1107–1111 (2012).
50. Hsieh, E. et al. Medication use in the neonatal intensive care unit. *Am. J. Perinatol.* **31**, 811–822 (2013).
51. Jia, B. et al. CARD 2017: expansion and model-centric curation of the comprehensive antibiotic resistance database. *Nucleic Acids Res.* **45**, D566–D573 (2017).
52. Crofts, T. S., Gasparrini, A. J. & Dantas, G. Next-generation approaches to understand and combat the antibiotic resistome. *Nat. Rev. Microbiol.* **15**, 422–434 (2017).
53. Wyres, K. L. & Holt, K. E. *Klebsiella pneumoniae* as a key trafficker of drug resistance genes from environmental to clinically important bacteria. *Curr. Opin. Microbiol.* **45**, 131–139 (2018).
54. Navon-Venezia, S., Kondratyeva, K. & Carattoli, A. *Klebsiella pneumoniae*: a major worldwide source and shuttle for antibiotic resistance. *FEMS Microbiol. Rev.* **41**, 252–275 (2017).
55. Goldstone, R. J. & Smith, D. G. E. A population genomics approach to exploiting the accessory 'resistome' of *Escherichia coli*. *Microb. Genom.* **3**, e000108 (2017).
56. Kaminski, J. et al. High-specificity targeted functional profiling in microbial communities with ShortBRED. *PLoS Comput. Biol.* **11**, e1004557 (2015).
57. Breiman, L. Random Forests. *Mach. Learn.* **45**, 5–32 (2001).
58. Carl, M. A. et al. Sepsis from the gut: the enteric habitat of bacteria that cause late-onset neonatal bloodstream infections. *Clin. Infect. Dis.* **58**, 1211–1218 (2014).
59. Zhang, X., Feng, Y., Zhou, W., McNally, A. & Zong, Z. Cryptic transmission of ST405 *Escherichia coli* carrying *bla*_{NDM-4} in hospital. *Sci. Rep.* **8**, 390 (2018).
60. Izdebski, R. et al. MLST reveals potentially high-risk international clones of *Enterobacter cloacae*. *J. Antimicrob. Chemother.* **70**, 48–56 (2015).
61. Gurnee, E. A. et al. Gut colonization of healthy children and their mothers with pathogenic ciprofloxacin-resistant *Escherichia coli*. *J. Infect. Dis.* **212**, 1862–1868 (2015).
62. Kim, H. B. et al. *oqxAB* encoding a multidrug efflux pump in human clinical isolates of Enterobacteriaceae. *Antimicrob. Agents Chemother.* **53**, 3582–3584 (2009).

63. Fevre, C., Passet, V., Weill, F.-X., Grimont, P. A. D. & Brisse, S. Variants of the *Klebsiella pneumoniae* OKP Chromosomal beta-lactamase are divided into two main groups, OKP-A and OKP-B. *Antimicrob. Agents Chemother.* **49**, 5149–5152 (2005).
64. Gasparini, A. J. et al. Antibiotic perturbation of the preterm infant gut microbiome and resistome. *Gut Microbes* **7**, 443–449 (2016).
65. Furtado, I. et al. *Enterococcus faecium* and *Enterococcus faecalis* in blood of newborns with suspected nosocomial infection. *Rev. Inst. Med. Trop. Sao Paulo* **56**, 77–80 (2014).
66. Akturk, H. et al. Vancomycin resistant *Enterococci* colonization in a neonatal intensive care unit: who will be infected? *J. Matern. Fetal Neonatal Med.* **29**, 3478–3482 (2016).
67. Brooks, B. et al. Microbes in the neonatal intensive care unit resemble those found in the gut of premature infants. *Microbiome* **2**, 1 (2014).
68. Fernández-Canigia, L., Cejas, D., Gutkind, G. & Radice, M. Detection and genetic characterization of β -lactamases in *Prevotella intermedia* and *Prevotella nigrescens* isolated from oral cavity infections and peritonsillar abscesses. *Anaerobe* **33**, 8–13 (2015).
69. Singh, B. et al. Probiotics for preterm infants: a national retrospective cohort study. *J. Perinatol.* **39**, 533–539 (2019).
70. Kerr-Wilson, C. O., Mackay, D. F., Smith, G. C. S. & Pell, J. P. Meta-analysis of the association between preterm delivery and intelligence. *J. Publ. Health* **34**, 209–216 (2012).
71. Johnson, S. et al. Academic attainment and special educational needs in extremely preterm children at 11 years of age: the EPICure study. *Arch. Dis. Child. Fetal Neonatal Ed.* **94**, F283–F289 (2009).
72. Bhutta, A. T., Cleves, M. A., Casey, P. H., Cradock, M. M. & Anand, K. J. S. Cognitive and behavioral outcomes of school-aged children who were born preterm: a meta-analysis. *JAMA* **288**, 728–737 (2002).
73. Tinnion, R., Gillone, J., Cheatham, T. & Embleton, N. Preterm birth and subsequent insulin sensitivity: a systematic review. *Arch. Dis. Child.* **99**, 362–368 (2014).
74. Parkinson, J. R. C., Hyde, M. J., Gale, C., Santhakumaran, S. & Modi, N. Preterm birth and the metabolic syndrome in adult life: a systematic review and meta-analysis. *Pediatrics* **131**, e1240–e1263 (2013).
75. Crump, C., Winkleby, M. A., Sundquist, K. & Sundquist, J. Risk of hypertension among young adults who were born preterm: a Swedish national study of 636,000 births. *Am. J. Epidemiol.* **173**, 797–803 (2011).
76. Kowalski, R. R. et al. Elevated blood pressure with reduced left ventricular and aortic dimensions in adolescents born extremely preterm. *J. Pediatr.* **172**, 75–80 (2016).
77. Crump, C., Winkleby, M. A., Sundquist, J. & Sundquist, K. Risk of asthma in young adults who were born preterm: a Swedish national cohort study. *Pediatrics* **127**, e913–e920 (2011).
78. Lum, S. et al. Nature and severity of lung function abnormalities in extremely pre-term children at 11 years of age. *Eur. Respir. J.* **37**, 1199–1207 (2011).
79. La Rosa, P. S. et al. Patterned progression of bacterial populations in the premature infant gut. *Proc. Natl Acad. Sci. USA* **111**, 12522–12527 (2014).
80. Planer, J. D. et al. Development of the gut microbiota and mucosal IgA responses in twins and gnotobiotic mice. *Nature* **534**, 263–266 (2016).
81. Baym, M. et al. Inexpensive multiplexed library preparation for megabase-sized genomes. *PLoS ONE* **10**, e0128036 (2015).
82. Bolger, A. M., Lohse, M. & Usadel, B. Trimmomatic: a flexible trimmer for Illumina sequence data. *Bioinformatics* **30**, 2114–2120 (2014).
83. Zhu, W., Lomsadze, A. & Borodovsky, M. Ab initio gene identification in metagenomic sequences. *Nucleic Acids Res.* **38**, e132 (2010).
84. Gibson, M. K., Forsberg, K. J. & Dantas, G. Improved annotation of antibiotic resistance determinants reveals microbial resistomes cluster by ecology. *ISME J.* **9**, 207–216 (2015).
85. Finn, R. D., Clements, J. & Eddy, S. R. HMMER web server: interactive sequence similarity searching. *Nucleic Acids Res.* **39**, W29–W37 (2011).
86. Altschul, S. F., Gish, W., Miller, W., Myers, E. W. & Lipman, D. J. Basic local alignment search tool. *J. Mol. Biol.* **215**, 403–410 (1990).
87. Rice, P., Longden, I. & Bleasby, A. EMBOSS: the European molecular biology open software suite. *Trends Genet.* **16**, 276–277 (2000).
88. Schmieder, R. & Edwards, R. Fast identification and removal of sequence contamination from genomic and metagenomic datasets. *PLoS ONE* **6**, e17288 (2011).
89. Bankevich, A. et al. SPAdes: a new genome assembly algorithm and its applications to single-cell sequencing. *J. Comput. Biol.* **19**, 455–477 (2012).
90. Gurevich, A., Saveliev, V., Vyahhi, N. & Tesler, G. QUAST: quality assessment tool for genome assemblies. *Bioinformatics* **29**, 1072–1075 (2013).
91. Seemann, T. Prokka: rapid prokaryotic genome annotation. *Bioinformatics* **30**, 2068–2069 (2014).
92. Ondov, B. D. et al. Mash: fast genome and metagenome distance estimation using MinHash. *Genome Biol.* **17**, 132 (2016).
93. Page, A. J. et al. Roary: rapid large-scale prokaryote pan genome analysis. *Bioinformatics* **31**, 3691–3693 (2015).
94. Mohamed, J. A., Huang, W., Nallapareddy, S. R., Teng, F. & Murray, B. E. Influence of origin of isolates, especially endocarditis isolates, and various genes on biofilm formation by *enterococcus faecalis*. *Infect. Immun.* **72**, 3658–3663 (2004).

Acknowledgements

This work is supported in part by awards to G.D. through the National Institute of General Medical Sciences of the National Institutes of Health (R01 GM099538), the National Institute of Allergy and Infectious Diseases of the National Institutes of Health (R01 AI123394) and the US Centers for Disease Control and Prevention (200-2016-91955); to P.I.T. through the National Institutes of Health (5P30 DK052574 (Biobank, DDRCC)); to G.D., P.I.T. and B.B.W. through the Eunice Kennedy Shriver National Institute Of Child Health and Human Development of the National Institutes of Health (R01 HD092414); to P.I.T. and B.B.W. through the Children's Discovery Institute at St Louis Children's Hospital and Washington University School of Medicine; and to A.J.G. through a NIGMS training grant award number T32 GM007067 (J. Skeath, principal investigator) and from the NIDDK Pediatric Gastroenterology Research Training Program award number T32 DK077653 (P.I.T., principal investigator). The content is solely the responsibility of the authors and does not necessarily represent the official views of the funding agencies. We thank members of the Dantas laboratory for helpful discussion of the manuscript, and staff from the Edison Family Center for Genome Sciences & Systems Biology, E. Martin, B. Koebbe and J. Hoisington-López for technical support and sequencing expertise.

Author contributions

A.J.G. and G.D. conceived and designed the study. P.I.T., B.B.W. and I.M.N. assembled the cohorts, collected the specimens and biological data and maintained the database, oversaw the transfer of specimens and clinical metadata and provided clinical insights. A.J.G. and B.W. extracted metagenomic DNA from stools and prepared shotgun metagenomic sequencing libraries. A.J.G., B.W. and A.H.-L. performed stool culturing experiments and isolate genomic DNA extraction. A.J.G. and B.W. prepared isolate genome sequencing libraries. E.A.K. performed *Enterococcus* phenotyping experiments. X.S. created functional metagenomic libraries, performed functional selections and prepared functional metagenomic sequencing libraries. A.J.G. analysed clinical metadata, shotgun metagenomic sequencing data, isolate genome sequencing data and functional metagenomic data. A.J.G. wrote the manuscript with input from G.D., B.B.W. and P.I.T.

Competing interests

P.I.T. is a member of the Scientific Advisory Board of, holds equity in and is a consultant to MediBeacon. P.I.T. is a coinventor on a filed patent application (US Patent application no. 16/200353) to test intestinal permeability in humans that might generate royalty payments. This involvement is not directly relevant to this manuscript. P.I.T. is also a consultant to Takeda Pharmaceuticals on pediatric gastrointestinal disorders and to the Bill & Melinda Gates Foundation on neonatal infections.

Additional information

Supplementary information is available for this paper at <https://doi.org/10.1038/s41564-019-0550-2>.

Reprints and permissions information is available at www.nature.com/reprints.

Correspondence and requests for materials should be addressed to G.D.

Publisher's note: Springer Nature remains neutral with regard to jurisdictional claims in published maps and institutional affiliations.

© The Author(s), under exclusive licence to Springer Nature Limited 2019

Reporting Summary

Nature Research wishes to improve the reproducibility of the work that we publish. This form provides structure for consistency and transparency in reporting. For further information on Nature Research policies, see [Authors & Referees](#) and the [Editorial Policy Checklist](#).

Statistical parameters

When statistical analyses are reported, confirm that the following items are present in the relevant location (e.g. figure legend, table legend, main text, or Methods section).

n/a Confirmed

- ☒ ☐ The exact sample size (n) for each experimental group/condition, given as a discrete number and unit of measurement
- ☐ ☒ An indication of whether measurements were taken from distinct samples or whether the same sample was measured repeatedly
- ☐ ☒ The statistical test(s) used AND whether they are one- or two-sided
Only common tests should be described solely by name; describe more complex techniques in the Methods section.
- ☐ ☒ A description of all covariates tested
- ☐ ☒ A description of any assumptions or corrections, such as tests of normality and adjustment for multiple comparisons
- ☐ ☒ A full description of the statistics including central tendency (e.g. means) or other basic estimates (e.g. regression coefficient) AND variation (e.g. standard deviation) or associated estimates of uncertainty (e.g. confidence intervals)
- ☐ ☒ For null hypothesis testing, the test statistic (e.g. F , t , r) with confidence intervals, effect sizes, degrees of freedom and P value noted
Give P values as exact values whenever suitable.
- ☒ ☐ For Bayesian analysis, information on the choice of priors and Markov chain Monte Carlo settings
- ☒ ☐ For hierarchical and complex designs, identification of the appropriate level for tests and full reporting of outcomes
- ☒ ☐ Estimates of effect sizes (e.g. Cohen's d , Pearson's r), indicating how they were calculated
- ☐ ☒ Clearly defined error bars
State explicitly what error bars represent (e.g. SD, SE, CI)

Our web collection on [statistics for biologists](#) may be useful.

Software and code

Policy information about [availability of computer code](#)

Data collection

No software was specifically used for data collection.

Data analysis

All of the applied software is cited in the Methods section. We list the tools here:

- Trimmomatic v0.36: quality filtering and adapter trimming
- DeconSeq v0.4.3: remove contaminating human DNA
- MetaPhlAn 2.0: metagenome taxonomic profiling
- HUMAnN2 v0.9.4: metagenome functional profiling
- PARFuMS: assembly of functionally selected fragments
- MetaGeneMark v3.2.6: gene prediction
- EMBOSS v6.6.0: global alignment
- SPAdes v3.11.0: genome assembly
- QUAST v4.5: assembly quality assessment
- Prokka v1.12: genome annotation
- Roary v3.8.0: pangenome analysis
- RAXML v8.2.11: maximum likelihood phylogeny construction
- Resfams: resistance gene annotation in functional selections
- Resfinder: resistance gene annotation in isolate genomes
- snp-dist: core genome SNP distance calculations
- HMMER3 v3.2.1: resistance gene annotation in functional selections

- ShortBRED: resistance gene quantification in metagenomes
- bbttools v38.26: short read alignment
- PRANK v1.0: core genome alignment:
- MLST v2.11: in silico MLST
- pyani v0.2.7: average nucleotide identity calculation
- R 3.5.2: statistical analysis

For manuscripts utilizing custom algorithms or software that are central to the research but not yet described in published literature, software must be made available to editors/reviewers upon request. We strongly encourage code deposition in a community repository (e.g. GitHub). See the Nature Research [guidelines for submitting code & software](#) for further information.

Data

Policy information about [availability of data](#)

All manuscripts must include a [data availability statement](#). This statement should provide the following information, where applicable:

- Accession codes, unique identifiers, or web links for publicly available datasets
- A list of figures that have associated raw data
- A description of any restrictions on data availability

Assembled functional metagenomic contigs, shotgun metagenomic reads, shotgun genomic reads, and assemblies have been deposited to NCBI GenBank and SRA under BioProject ID PRJNA489090.

Field-specific reporting

Please select the best fit for your research. If you are not sure, read the appropriate sections before making your selection.

☒ Life sciences ☐ Behavioural & social sciences ☐ Ecological, evolutionary & environmental sciences

For a reference copy of the document with all sections, see [nature.com/authors/policies/ReportingSummary-flat.pdf](https://www.nature.com/authors/policies/ReportingSummary-flat.pdf)

Life sciences study design

All studies must disclose on these points even when the disclosure is negative.

Sample size	Because this was a non-interventional, observational study that leveraged existing samples for which recruitment, enrollment, and sample collection had concluded and anticipated effect sizes were unclear, we did not perform a priori power calculations. We included all infants from whom post-discharge (follow up) samples were available.
Data exclusions	Subjects were enrolled without regard to race, gender, or ethnic statuses, proportional to neonatal patient populations. Because we were focused on early life development of the gut microbiota, we excluded samples from children older than 20 months of age from our study. These exclusion criteria were pre-established.
Replication	Enterococcus biofilm formation and antimicrobial susceptibility testing assays were performed in triplicate at a minimum, and all results were found to be reproducible across replicates.
Randomization	This work is a non-interventional observational study, so randomization of participants was not necessary.
Blinding	This work is a non-interventional observational study and investigators had no direct contact with participants, so blinding is not relevant.

Reporting for specific materials, systems and methods

Materials & experimental systems

n/a	Involved in the study
<input checked="" type="checkbox"/>	<input type="checkbox"/> Unique biological materials
<input checked="" type="checkbox"/>	<input type="checkbox"/> Antibodies
<input checked="" type="checkbox"/>	<input type="checkbox"/> Eukaryotic cell lines
<input checked="" type="checkbox"/>	<input type="checkbox"/> Palaeontology
<input checked="" type="checkbox"/>	<input type="checkbox"/> Animals and other organisms
<input type="checkbox"/>	<input checked="" type="checkbox"/> Human research participants

Methods

n/a	Involved in the study
<input checked="" type="checkbox"/>	<input type="checkbox"/> ChIP-seq
<input checked="" type="checkbox"/>	<input type="checkbox"/> Flow cytometry
<input checked="" type="checkbox"/>	<input type="checkbox"/> MRI-based neuroimaging

Human research participants

Policy information about [studies involving human research participants](#)

Population characteristics	<p>Study category: 9 preterm early only antibiotics, 32 early and subsequent antibiotics, 17 term antibiotic naive; sex: 23 male, 35 female; mode of delivery: 46 C-section, 12 vaginal.</p> <p>The characteristics of the study population are further detailed in Table 1 and Supplementary Table 1.</p>
Recruitment	<p>Samples and patient metadata proposed for use in this study are drawn from two prior studies:</p> <ol style="list-style-type: none">1. Dr. Barbara Warner’s “The St. Louis Neonatal Gut Microbiome Initiative” study, funded by Children’s Discovery Institute grant MD-II-2009-201, and approved by the Washington University IRB (HRPO #201105492).2. Dr. Phillip Tarr’s “The Neonatal Microbiome and Necrotizing Enterocolitis” study, funded by NIH grant UG3AI083265, and approved by the Washington University IRB (HRPO #201104267). <p>Both studies have completed recruitment, enrollment and sample collection. Initial consent included sample sharing with other investigators. No patients were specifically recruited for this study. Of infants meeting study criteria, 92% were enrolled (infants with major congenital anomalies and unlikely to survive the first week of life were not eligible).</p>